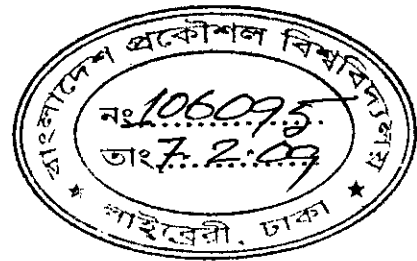


PERFORMANCE ANALYSIS OF AN ATMOSPHERIC OPTICAL M-
PPM CDMA SYSTEM WITH OPTICAL ORTHOGONAL CODE AND
PARTIAL MODIFIED PRIME CODE

A Thesis submitted to the Department of Electrical and Electronic Engineering in partial
fulfillment of the requirements for the degree of
Master of Science in Electrical and Electronic Engineering (EEE)

By

Jakir Hossen

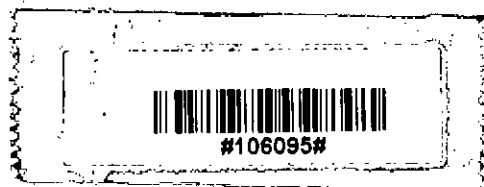


Under the supervision of
Professor Dr. S. P. Majumder




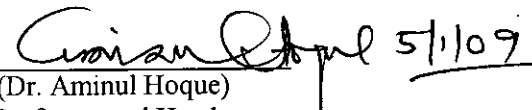
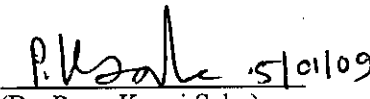
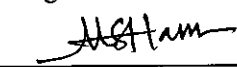

Department of Electrical and Electronic Engineering (EEE)
Bangladesh University of Engineering and Technology (BUET)
Dhaka, Bangladesh.

January 2009



The thesis titled “Performance analysis of an atmospheric optical M-PPM CDMA system with optical orthogonal code and modified prime code” submitted by Ja kir Hossen, Roll No. 040506231, Session “April 2005” has been accepted as satisfactory in partial fulfillment of the requirements for the degree of **Master of Science in Electrical and Electronic Engineering** on 05 January, 2009.

Board of Examiners

1. 
(Dr. Satya Prasad Majumder)
Professor,
Department of Electrical and Electronic Engineering,
Bangladesh University of Engineering and Technology,
Dhaka-1000
Bangladesh. Chairman
2. 
(Dr. Aminul Hoque)
Professor and Head
Department of Electrical and Electronic Engineering,
Bangladesh University of Engineering and Technology,
Dhaka-1000
Bangladesh. Member
(Ex-officio)
3. 
(Dr. Pran Kanai Saha)
Professor
Department of Electrical and Electronic Engineering,
Bangladesh University of Engineering and Technology,
Dhaka-1000
Bangladesh. Member
4. 
(Dr. Md. Shah Alam)
Associate Professor
Department of Electrical and Electronic Engineering,
Bangladesh University of Engineering and Technology,
Dhaka-1000
Bangladesh. Member
5. 
(Engr. Md. Abdul Moqaddem)
(M.Sc. Engg., BUET)
DGM, Teletalk Bangladesh Ltd.
House no. 41, Road-27, Block-A
Banani, Dhaka. Member
(External)

DECLARATION

It is hereby declared that this thesis “Performance analysis of an atmospheric optical M-PPM CDMA system with optical orthogonal code and modified prime code” any part of it has not been submitted else where for the award of any degree or diploma.

Signature of the candidate



.....
(Jakir Hossen)

Dedication

To my beloved parents

ACKNOWLEDGEMENT

This project is accomplished under the supervision of Dr. Satya Prasad Majumder, Professor and Ex-Head, Department of Electrical and Electronic Engineering, Bangladesh University of Engineering and Technology (BUET), Dhaka. It is a great pleasure to express the author's indebtedness gratitude and profound respect to his supervisor for the supervisor's consistent guidance, relentless encouragement, helpful suggestions, constructive criticism and endless patience throughout the progress of this research. The successful completion of this thesis would not have been possible without his persistent motivation and continuous guidance.

The author is also grateful to Dr. Aminul Hoque, professor and Head, Department of Electrical and Electronic Engineering, Bangladesh University of Engineering and Technology (BUET), Dhaka, for providing valuable suggestions on writing the thesis papers.

The author is also indebted to the librarian and other staffs of the Department of EEE for their help and co-operation in completing the project.

Finally, all praises to Allah, the most gracious benevolent, without Whose help this work would not have been possible.

CONTENTS

A. Approval	(i)
B. Declaration	(ii)
C. Dedication	(iii)
D. Acknowledgement	(iv)
E. Contents	(v)
F. Lists of Figures	(viii)
G. Lists of Tables	(x)
H. List of Important Abbreviation and Symbol	(xi)
I. Abstract	(xiii)

CHAPTER 1	General Introduction	
1.1	General Perspective	1
1.2	Advantages of Optical Wireless Communication	3
1.3	Brief History of Optical Communication System	4
1.4	Recent Optical Wireless Communication Systems	5
1.4.1	Indoor Application	5
1.4.2	Outdoor Application	6
1.5	Literature Review	7
1.6	Objective of this thesis work	8

CHAPTER 2 **Optical Wireless Communication Systems**

2.1 Introduction of Optical Wireless Communication Systems	9
2.2 Optical Wireless Links	11
2.3 Major Components of Optical Wireless Link	12
2.3.1 Optical Sources	13
2.3.1.1 Light emitting diode (LED)	13
2.3.1.2 LASER	13
2.3.2 Optical detectors	14
2.3.2.1 PIN diode	14
2.3.2.2 Avalanche photo diode (APD)	15
2.4 IM/DD Channels	15
2.5 Design of Power Efficient Links	18
2.6 Optical Transmitter and Eye Safety	18

CHAPTER 3 **Analysis of Optical Code Division Multiple Access (OCDMA) Transmission System**

3.1 The principle of spread spectrum	22
3.2 Radio frequency communications spread spectrum techniques	23
3.2.1 Direct sequence spread spectrum	23
3.2.2 Frequency hopped spread spectrum	26
3.3 Spread spectrum as a multiple access techniques	27
3.4 Orthogonal Multiple Access	28
3.4.1 Orthogonal Codes	28
3.5 Non-orthogonal Multiple Access	29
3.5.1 m-Sequence	29
3.5.1.1 Properties of m-sequence	30
3.5.2 Gold Sequence	33
3.5.3 Prime code	35
3.5.3.1 Construction of partial modified prime codes (PMP)	36

**CHAPTER 4 Performance Analysis of an Atmospheric Optical M-PPM
CDMA system**

4.1 Introduction	41
4.2 Signal Current at the Output of an Optical Direct Detection Receiver	41
4.3 Receiver Output Statistics	41
4.4 Performance Analysis with Atmospheric Scintillation	42

CHAPTER 5 Results and Discussion

5.1 Introduction	50
5.2 Results and Discussion	50

CHAPTER 6 Conclusions

6.1 Conclusion	69
6.2 Further Scope of Works	70

References	71
-------------------	----

Appendices

APPENDIX A: Simplification of Probability Bit Error Rate (BER) for M-PPM	78
APPENDIX B: HERMITE POLYNOMA	82

List of Figures

Fig.1.1	Integration of radio and optical communication	3
Fig.1.2	An indoor wireless optical communication system.	5
Fig.1.3	Wide-area overlay networks	6
Fig.2.1	LOS link Transmitter and Receiver	11
Fig.2.2	Basic Optical Wireless Communication Link	12
Fig.2.3	Modeling Link as a baseband filter, time-invariant system having impulse response $h(t)$, with signal-independent, additive noise $N(t)$. The photodetector has responsivity R	16
Fig.3.1 (a)	Direct Sequence spread Spectrum Block Diagram (Transmitter)	24
Fig.3.1 (b)	Direct Sequence spread Spectrum Block Diagram (Receiver)	24
Fig.3.2	Spread spectrum modulation in time domain	25
Fig.3.3	Spread spectrum demodulation in time domain	25
Fig.3.4	Hardware of a pseudo-noise (PN) generator	30
Fig.3.5	Auto correlation of 7 chip m-sequence with shift 1	32
Fig.3.6	Block diagram of Gold Sequence Generator	34
Fig.3.7	An exemplary procedure for generating $(0, 1)$ sequence $C_{x,r,m}$ based on the partial modified prime sequence $S_{x,r,m}$	39
Fig.4.1	Model of atmospheric optical CDMA systems.	43
Fig.4.2	Block diagram of a PPM/CDMA transmitter and signaling format for the x th user, $L=13$, $k=3$ and $A^x = (1,1,0,0,1,0,0,0,0,0,0,0,0)$.	44
Fig.4.3	Block diagram of a PPM/CDMA receiver	44
Fig.4.4 (a)	Sequence Encoder and (b) Optical correlator for the x th user $L=13$, $k=3$ and $A^x = (1,1,0,0,1,0,0,0,0,0,0,0,0)$.	44
Fig.4.5	Sample bit stream in PPM modulation formats.	45
Fig.5.1	BER Versus the received laser power without scintillation P_w for four-ary PPM CDMA ($M=4$, $\sigma_s^2=0$, $\sigma_x^2=0.005$)	52
Fig.5.2	BER Versus the received laser power without scintillation P_w for four-ary PPM CDMA ($M=4$, $\sigma_s^2=0.01$)	53

Fig.5.3	BER Versus the received laser power without scintillation P_w for M-ary PPM CDMA ($\sigma_s^2=0$)	54
Fig.5.4	BER Versus the average received laser power without scintillation P_w for M-ary PPM CDMA ($\sigma_s^2=0.1$)	55
Fig.5.5	BER Versus the received laser power without scintillation P_w for four-ary PPM CDMA in the presence of different values of σ_s^2	56
Fig.5.6	Power penalty as a function of variance of scintillation (M=4)	57
Fig.5.7	Power penalty as a function of variance of scintillation for M-ary PPM	58
Fig.5.8	BER Versus Number of Users for M-ary PPM-CDMA ($\sigma_s^2 =0.001$)	59
Fig.5.9	BER Versus Number of Users for M-ary PPM-CDMA ($\sigma_s^2 =0.005$)	60
Fig.5.10	BER Versus Number of Users for M-ary PPM-CDMA ($\sigma_s^2 =0.01$)	61
Fig.5.11	BER Versus Number of Users for M-ary PPM-CDMA ($\sigma_s^2 =0.1$)	62
Fig.5.12	BER Versus the received laser power without scintillation P_w considering M-PPM CDMA system with OOC's and PMP codes (M=4, N=3, $\sigma_s^2 =0.1$)	63
Fig.5.13	BER Versus the received laser power without scintillation P_w considering M-PPM CDMA system with OOC's and PMP codes in the presence of different values of σ_s^2 (M=2, N=3)	64
Fig.5.14	BER Versus the received laser power without scintillation P_w considering M-PPM CDMA system with OOC's and PMP codes in the presence of different values of σ_s^2 (M=4, N=3)	65
Fig.5.15	BER Versus the received laser power without scintillation P_w considering M-PPM CDMA system with OOC's and PMP codes in the presence of different values of σ_s^2 (M=8, N=3)	66
Fig.5.16	BER Versus the received laser power without scintillation P_w considering M-PPM CDMA system with OOC's and PMP codes in the presence of different values of σ_s^2 (M=16, N=3)	67
Fig.5.17	BER versus the number of active users for OCDMA systems with PMP codes	68

Lists of Tables

Table 2.1 Comparison between radio and IM/DD optical wireless systems	10
Table 2.2 Comparison between LED's and LD's	19
Table 3.1 Numerical values are illustrated in table	31
Table 3.2 Reference Sequence: 1110010	33
Table 3.3 Example of the Modified Prime Codes for GF (5)	37
Table 3.4 Example of the Partial Modified Prime Codes for GF (5) and M=2	40
Table 5.1 Nominal Parameters of Optical Wireless Communication Link	51

List of Important Abbreviation and Symbol

MPPM	M-ary Pulse Position Modulation
BER	Bit Error Rate
APD	Avalanche Photo Diode
EMI	Electro-Magnetic Interference
ISI	Inter Symbol Interference
FOV	Focus of Vision
ROF	Radio on Fiber
UART	Universal Asynchronous Receiver Transreceiver
OBN	Optical Beam Networking
IEEE	International Electrical and Electronic Engineer
MUI	Multi User Interference
MAI	Multi Access Interference
PIIN	Phase Induced Intensity Noise
WDM	Wave Length Division Multiplexing
IM	Intensity Modulation
DD	Direct Detection
CDMA	Code Division Multiple Access
LED	Light Emitting Diode
LASER	Light Amplification by Stimulated Emission of Radition
IEC	International Electro-technical Commission
LOS	Line of Sight
CSC	Correct Slot Choice
OOC	Optical Orthogonal Code
PMP	Partial Modified Prime Code
PIN	Positives Intrinsic Negative

σ_s^2	Scintillation
P_b	Background Noise
λ	Wavelength
T_r	Receiver Noise Temperature
I_s	Surface Leakage current
I_b	Bulk Leakage Current
B_r	Bit Rate
k_{eff}	APD effective Ionization Ratio

ABSTRACT

The growth in mobile and portable computing within recent years has led to an increasing demand for wireless data connectivity. Direct Detection Laser communication systems are potentially very promising for future deep space application, inter-satellite optical links and terrestrial line of sight communication. It has been researched widely in recent years due to increasing interest in laser satellite-ground links and urban optical wireless communication. The major source of performance degradation have been identified as the atmospheric molecular absorption, aerosol scattering and turbulence. The primary factor affecting the performance of the systems is intensity fluctuation that is known as the log-normal intensity scintillation. In optical CDMA systems, multi-user interference is one of the most serious problems. In this thesis a theoretical analysis is provided to evaluate the performance of an optical M-ary Pulse Position Modulation (MPPM) taking into account the effects of Scintillation, avalanche photodiode noise, thermal noise and multi-user interference. The expression for the signal current at the output of an optical direct detection receiver with sequence inverse keying operation considering the effect of scintillations is derived. The analysis is extended to find the expression for multi-access interference (MAI) and that of signal to MAI ratio. The expression of probability of bit error is derived conditioned on a given value of atmospheric scintillation. Using the probability density function of the atmospheric scintillation, the average bit error rate is derived. The result is evaluated by numerical computations considering the system with optical orthogonal code (OOC) and partial modified prime code (PMP). The effect of atmospheric scintillation on the Bit error rate (BER) performance is determined in the forms of power penalty and the results are compared for OOC's and PMP codes and optimum system parameters are determined.

Chapter 1

General Introduction



1.1 General Perspective

The growth in mobile and portable computing within recent years has led to an increasing demand for wireless data connectivity. Trends in the telecommunications and computer industries suggest that the network of the future will consist of a high capacity backbone network with short range communication links providing network access to portable communications and portable computers. The next generation network environment will be constructed of the high-capacity backbone network and a large number of access networks. In order to realize such access networks, high speed wireless networks are required. In this vision of the future, mobile users will access to similar grade high-speed network services available to wired terminals. For this purpose, some parts of communication links need to be constructed wireless. This situation is illustrated in Fig. 1.1. During the last decade, therefore, the wireless communication technology has grown rapidly[1-4]. The technology base for implementing this concept does not yet exist, however, Radio technology, although well-suited for moderate-speed applications. To illustrate the potential capacity requirements of a wireless network, consider the needs of a portable high-quality digital display. To reduce its size, weight, battery-power consumption, and cost, it may be advantageous to make it simple as possible, having little on-board computational power, and relegating intensive signal processing tasks such as video decompression to the transmitter platform. To accomplish this, however, it will require mid-range or short-range wireless communication link switch with extremely high capacity. In an extreme case, for example, uncompressed high-definition video can require a data rate of 100Mbit/s[5-6].

An optical wireless communication system is an attractive alternative to radio, primarily because of a virtually unlimited, unregulated bandwidth[7]. The optical spectrum is a universally available resource without frequency and wavelength regulations. An optical wireless communication system i.e. the infrared (IR) medium has the advantages of requiring low-cost and low power-consumption components, being spectrally unregulated and providing potentially very high data rates[8]. Moreover, for indoor applications, optical radiation is confined within a room since the radiation is either reflected or absorbed by the walls because of its short wavelength. Therefore cell planning in networks is simple and easy. In the near future, optical wireless communication system will be an attractive candidate for wireless access network.

From the view of the integration of radio and optical technology, on the other hand, an optical wireless communication technology is the important issue. Conventionally, the radio wave has been considered to be a technology for free space communication, and light wave has been considered to be a technology for an optical fiber. Integrated technologies of radio and optical, however, are attracting the attention in recent years. This is illustrated in Fig.1.1. Radio on fiber (ROF) technology is the technology for letting a radio wave pass through an optical fiber. This technology makes it possible that the data from many mobile users can be sent in an optical fiber directly. In an optical wireless communication technology, the light wave which has been considered to be for a wired connection is emitted in to the air. High capacity wireless transmission is possible in an optical wireless technology. Thus, an optical wireless communication technology is considered to be an important technique as an integration of radio and optical technology.

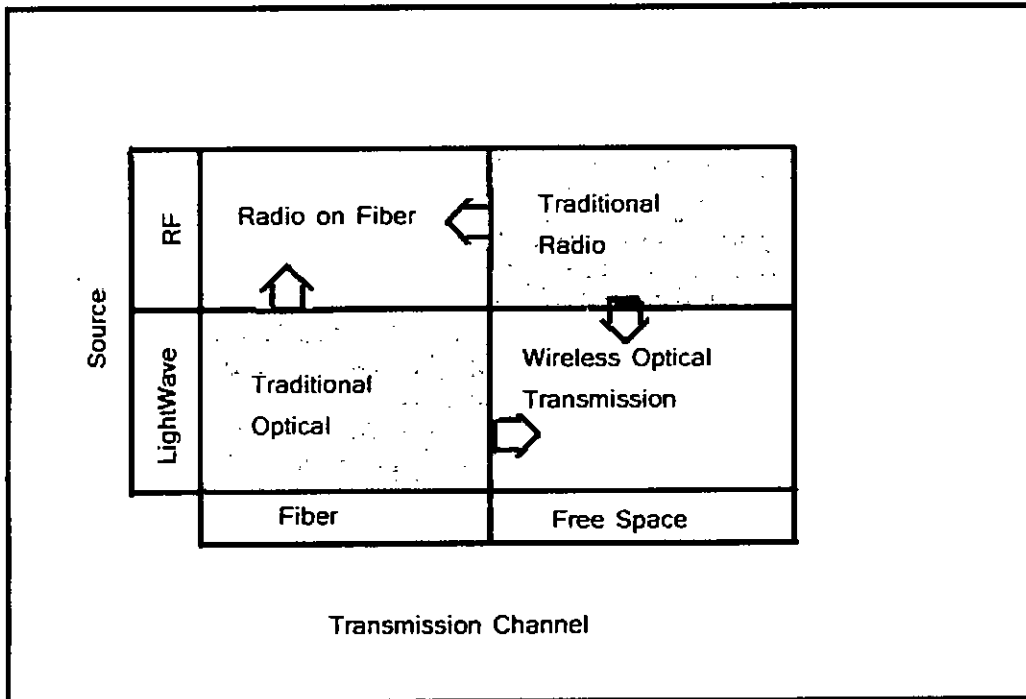


Fig.1.1. Integration of radio and optical communication

1.2 Advantage of Optical Wireless communication

As a method of realizing high speed wireless networks, the optical wireless communication systems are capturing the spotlight, on the other hand. Optical wireless communication systems have the following various advantages compared with radio systems.

1. An optical carrier has wide bandwidth available and is suitable for high speed communication networks.
2. The devices for an optical wireless transmission system are low in cost. Also no cable or fiber is needed for transmission. Thus the optical wireless communications system is suited for a consumer communication networks.
3. A lightwave cannot penetrate the opaque object such as walls. It is thought that the light wave is secured against eavesdropping. Therefore cell planning in networks is simple and easy.
4. The optical wireless networks occupy no radio frequency spectrum and it can be used where electro-magnetic interference is strictly prohibited, such as in hospital, airplanes and so on.
5. The lightwaves are worldwide unregulated by any law.

1.3 Brief History of Optical Communication system

Optical communication systems date back two centuries, to the “optical telegraph” that French engineer Claude Chappe invented in the 1790’s[9]. His system was a series of semaphores mounted on towers, where human operators relayed messages from one tower to the next. It beat hand-carried messages hands down, but by mid-19th century was replaced by the electric telegraph, leaving a scattering of “Telegraph Hills” as its most visible legacy. After passing long time, the optical fiber was invented. Optical fiber depended on the phenomenon of total internal reflection, which can confine light in a material surrounded by other materials with lower refractive index, such as glass in air. In the 20th century, inventors realized that bent quartz rods could carry light, and optical fibers went a step further. They are essentially transparent rods of glass or plastic stretched so they are long and flexible. They were used for a image-transmission by doctors in the incipient stage. The goal was to look inside inaccessible parts of the body.

On the other hand, optical transmission came to be available for the communication system after the laser as a light source was invented. As a coherent light source being not in a nature, ruby laser was invented by Dr. T Mainman in 1960, He-Ne laser oscilated in Bel labs next year, and GaAs semiconductor laser oscillated in 1962. The continuous oscillation of GaAlAs laser was realized in Japan, the united states and the Soviet Union in 1970, and the small semiconductor technology greatly. Around from 1965, the beam guide system which arranged the lens in a pipe, and the space propagation system which emits light to free space were beginning to be studied so as to use laser for free space optical communication[10]. In 1979, indoor optical wireless communication system has been presented by F. R. Gfeller and U. Bapst. In their system, diffuse optical radiation in the near-infrared region was utilized s signal carrier to interconnect a cluster of terminals located in the invention of continuous semiconductor laser has moved the mainstream of the research to optical fiber transmission, and the utilization of optical transmission system was accelerated from 1970 to 1980.

1.4 Recent Optical Wireless Communication Systems

In the 1990s, some practical applications using optical wireless communication got actual shape, and some products and their standards were completed. Optical wireless systems are classified into two categories depending on where the system is utilized. In this section, these applications will be introduced from this point of view.

1.4.1 Indoor applications

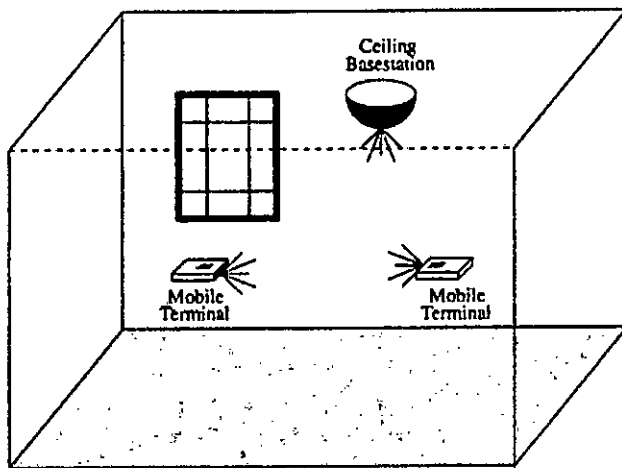


Fig.1.2 An indoor wireless optical communication system.

There is a growing interest in indoor wireless networks as a consequence of the large scale utilization of personal computers and mobile communications in Fig.1.2[78]. In this application, an optical wireless communication system is a candidate for the media of wireless networks. Infrared is preferred as wavelength in these applications originally. This is because essentially a large total transmission bandwidth is possible, facilitating fast transmission systems due to the very high frequency involved in optical carrier[2]. Moreover, because of the short wave length, optical radiation is confined within a room since the radiation is either reflected or absorbed by the walls. Therefore cell planning in networks is simple.

1.4.2 Outdoor applications

Wide-area Overlay Networks

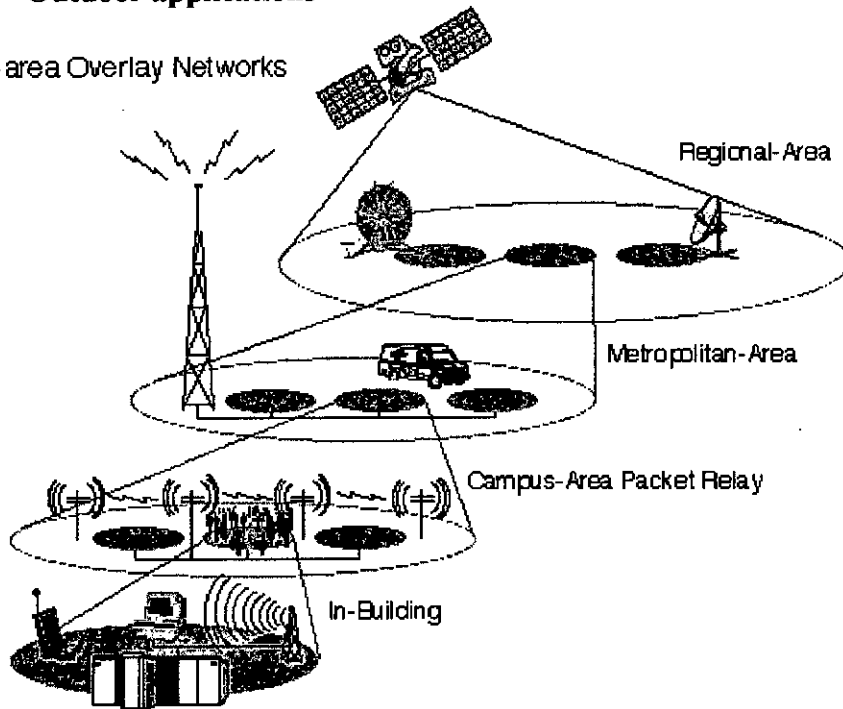


Fig.1.3 Wide-area overlay networks

Fig.1.3 presents a diagram of a typical indoor wireless optical communications scenario. There are many situations where an optical fiber is not always suitable for a fixed link, examples include temporary links, rapid deployment requirements and extremely cost sensitive links such as that from the curb to the house. The cost problem in the links such as that from the curb to the house is called “last one mile problem” in particular. Radio and microwave links currently solve some of these issues, however such systems are not without some serious drawbacks, notably high cost, large physical size, the need for regulatory approval and spectrum allocation, and the low bandwidth available. Optical wireless systems can be utilized in these situations also.

Over long distance (1 to 5km) optical wireless solutions can offer very rapid provision of exceedingly high bandwidth at least 1 to 10 Gbit/s is easily achievable. This flexibility is brought at the price of increased downtime, due to occasionally unfavorable atmospheric conditions, but would be invaluable where bandwidth was either needed very rapidly, say for disaster recovery, or only temporarily, say at a sporting event.

1.5 Literature Review

Optical wireless Communication is attractive more and more attention because of its ability to provide increased capacity, lower cost and flexibility. It becomes very popular in terrestrial application as well as in inter-satellite to ground communication[36, 37] and also the places where fiber can't be installed very easily but large volume of data needs to be transferred. It can be used as information bridges between buildings containing cables or wireless subnet. When the atmosphere forms part of the propagation channel, scintillation, multi-scattering phenomena are recognized as being the major source of communication performance degradation, leading to link failure and system downtime.

As a multiple access technique in optical communication, optical code-division multiple-access (CDMA) schemes have attracted much attention, particularly in the field of fiber-optic networks, because they allow multiple users to access the network asynchronously and/or simultaneously[15]. Higher order PPM offers better performance than on-off keying (OOK) at a given BER[16-19]. Optical CDMA is advantageous in that it makes channel assignment easier than in time-division multiple-access (TDMA) or frequency-division multiple-access (FDMA) systems. Thus, optical CDMA is an attractive option for future optical access networks[20].

The performance of atmospheric optical systems is strongly influenced by atmospheric molecular absorption, aerosol scattering and turbulence[20]. These influences can be specified by the attenuation and the fluctuation of the received optical power. In the atmospheric optical communication system using intensity modulation and direct-detection (IM/DD) the primary factors affecting the performance of the systems is intensity fluctuation that is known as the log-normal intensity scintillation. In optical CDMA systems, multi-user interference is one of the most serious problems. It is important to analyze the performance of an optical CDMA system over a free space optical link considering the above system limitation. However the effect of atmospheric scintillation on the BER performance in the forms of power penalty and the results compare for different types of codes are yet to reported (known to authors).

1.6 Objectives of this thesis work:

- * To carry out analysis for evaluating the Bit-error rate performance of an optical M-PPM CDMA system.
- * To extend the analysis to include the effect of atmospheric Scintillations in an M-PPM optical CDMA system.
- * To derive a closed form analytical expression of Bit error rate for optical M-PPM CDMA system with OOC and PMP codes considering Scintillation.
- * To evaluate the performance results by numerical computations.
- * To find out improvement in system performance in terms of power penalty due to scintillation effect.
- * To compare the performance results for different numbers of M of M-ary PPM.
- * To compare the performance results of the system with different codes: OOC code and PMP code.

Chapter 2

Optical Wireless Communication System

2.1 Introduction of Optical Wireless Communication System

As a medium for wireless communication, lightwave radiation offers several significant advantages over radio. Lightwave emitters and detectors capable of high speed operation are available at low cost. The lightwave spectral region offers a virtually unlimited bandwidth that is unregulated worldwide. Infrared and visible light are close together in wavelength, and they exhibit qualitatively similar behavior. Both are absorbed by dark objects, diffusely reflected by light-colored objects and directionally reflected from shiny surface, both types of light penetrate through glass, but not through walls or other opaque barriers, so that optical wireless transmission are confined to the room in which they originate. This signal confinement makes it easy to secure transmissions against casual eavesdropping, and it prevents interference between links operating in different rooms. Thus, optical wireless networks can potentially achieve a very high aggregate capacity, and their design may be simplified, since transmission in different rooms need not be coordinated. When an optical wireless link employs intensity modulation with direct-detection (IM/DD), the short carrier wavelength and large-area square-law detector lead to efficient spatial diversity that prevents multipath fading. By contrast, radio links are typically subject to large fluctuations in received signal magnitude and phase. Freedom from multipath fading greatly simplifies the design of optical wireless links.

The lightwave is not without drawbacks however, Because light wave cannot penetrate walls, communication from one room to another requires the installation of optical wireless access point that are interconnected by wired backbone. In many applications, there exists intense ambient light noise, arising from sunlight, incandescent lighting and fluorescent lighting, which induce noise in an optical wireless receiver. In virtual al short-range, indoor applications, IM/DD is the only practical transmission technique. The signal to noise ratio (SNR) of a direct detection receiver is proportional to the square of the received optical power, implying that IM/DD links can tolerate only a comparatively

limited path loss. Often optical wireless link must employ relatively high transmit power levels and operate over a relatively limited range. While the transmitter power level can usually be increased without fear of interfering with other users, transmitter power may be limited by concerns of power consumption and eye safety, particularly in portable transmitters. The characteristics of radio and indoor optical wireless links are compared in Table 2.1

Table 2.1: Comparison between radio and IM/DD optical wireless systems

Property of Medium	Radio	IM/DD optical wireless
Bandwidth Regulated	Yes	No
Passes through wall	Yes	No
Multipath fading	Yes	No
Multipath distortion	Yes	Yes
Path loss	High	High
Dominant loss	Other users	Background light
Input X(t) represent	Amplitude	Power
SNR proportional to	$\int X(t) ^2 dt$	$\int X(t) ^2 dt$
Average power proportional to	$\int X(t) ^2 dt$	$\int X(t) dt$

Radio and lightwave are complementary transmission media, and different applications favor the use of either one medium or the other. Radio is favored in applications where user mobility must be maximized or transmission through walls or over long distance is required and may be favored when transmitter power consumption must be minimized. Lightwave is favored for short-range applications in which per-links bit rate and aggregate system capacity must be maximized, cost must be minimized, international compability is required, or receiver signal-processing complexity must be minimized.

2.2 Optical Wireless Links

Optical wireless links may employ various designs, and it is convenient to classify them according to two criteria. This classification schemes is shown in Fig.2.1[6]. The first criterion is the degree of directionality of the transmitters and receivers, which must be aimed in order to establish a link, while non-directed employ wide-range transmitters and receivers, alleviating the need for such pointing or tracking. Directed link design maximizes power efficiency, since it minimizes path loss and reception of ambient light noise. On the other hand, non directed links may be more convenient to use, particularly for mobile terminals, since they do not require aiming of the transmitter or receiver. It is also possible to establish hybrid links, which combine transmitters and receivers having different degrees of directionality. The second classification criterion relates to whether the link relies upon the existence of an uninterrupted line of sight (LOS) path between the transmitter and receiver. LOS links rely upon such a path, which non-LOS links generally rely upon reflection of light from the ceiling or some other diffusely reflecting surface. LOS links design increases link robustness and ease of use, allowing the link to operate even when barriers, such as people or cubicle partitions, stand between the transmitter and receiver. The greatest robustness and ease of use are achieved by the non-directed-non-LOS link design, which is often referred to as a diffuse link.

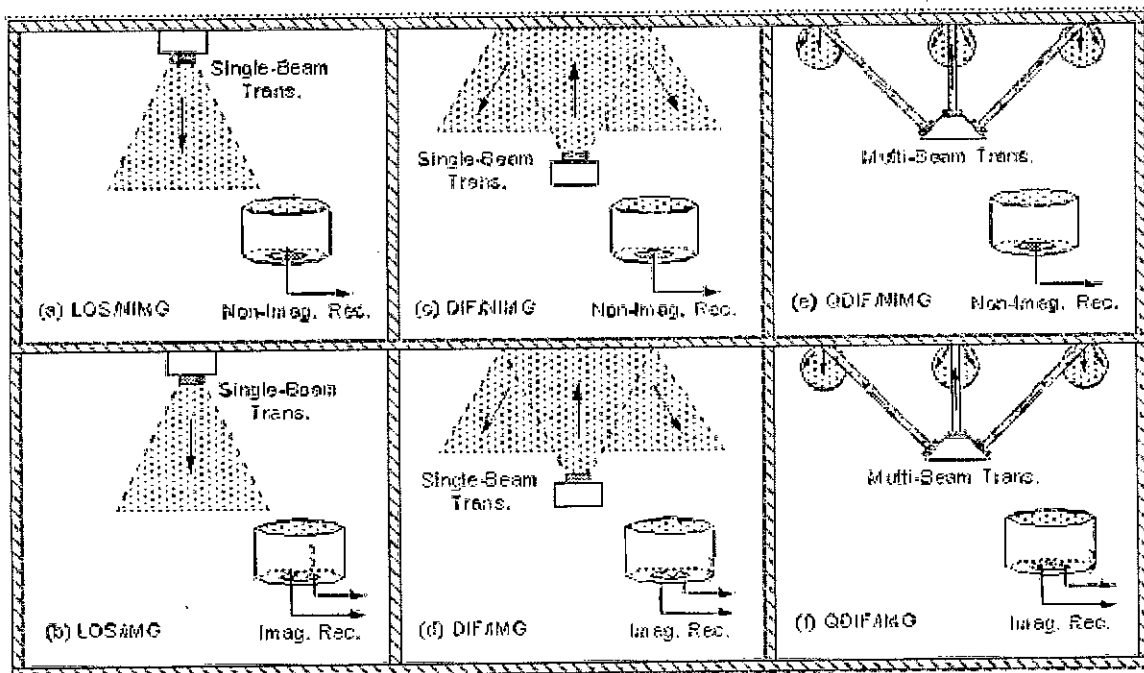


Fig 2.1 LOS link Transmitter and Receiver

In diffuse link, it is generated that a single path is always present, regardless of obstacles or people impeding the LOS path. This link also allows roaming to some degree. However, the penalty of diffuse transmission is a much reduced capacity compared with an LOS link. This is entirely a consequence of the multiple signal paths reaching the receiver, which cause classic pulse spreading and inter-symbol interference. Research has shown that the theoretical capacity of a diffuse system is a function of many factors such as room size and geometry, the fabric and distribution of furnishings and the placement and orientation of the base and user stations[76],[78]. Generalizing, this work predicts an upper bound of about 25 Mbit/s in a room 10m on each side, although higher rates have been demonstrated under particular conditions. Interference from ambient light is a particular issue for diffuse systems because of the extremely wide field of view of the receivers. However, the use of optical filters and robust signal formats minimizes any performance penalty that may arise. A decision feedback equalizer (DFE) or maximum likelihood sequence detection (MLSD) technique can improve the performance in a diffuse link also.

2.3 Major Components of Optical Wireless Link

An optical wireless links consists of a transmitter, wireless communication channels and a receiver as shown in Fig. 2.2.

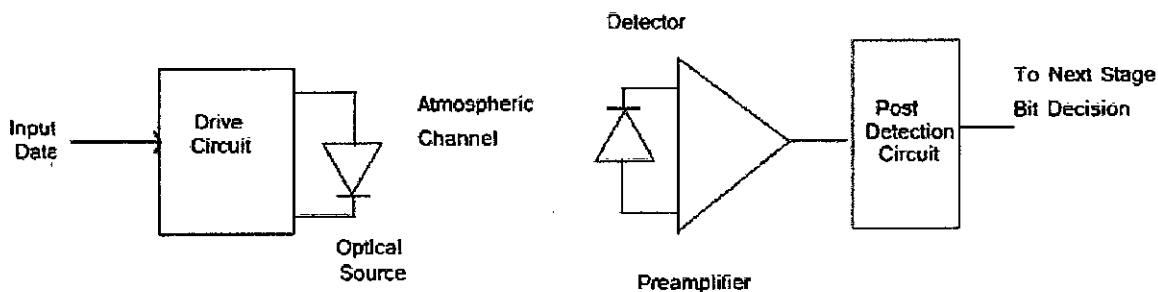


Fig. 2.2 Basic Optical Wireless Communication Link

2.3.1 Optical Source

In most optical communication systems, semiconductor light sources are used to convert electrical signals into light[11-12]. Optical sources for wireless transmission must be compatible to overcome the atmosphere effects and they should be such that one can easily modulate the light directly at high data rates. Generally either LASERs or LEDs are used in optical communication systems.

2.3.1.1 Light Emitting Diode (LED)

Light emitting diode (LEDs) used in optical communication system are the same as visual display LEDs except that they operate in the infrared region and with many times higher intensity of emission. When the p-n junction is forward biased, photon emission takes place due to recombination of electron-hole pair. The wavelength of emission will depend on the energy gap.

2.5.1.2 Laser

Laser stands for “Light amplification by stimulating emission of radiation”. Compared to LED, a laser has wider bandwidth, higher power output, higher modulation efficiency, narrower spectral line width and narrower emission pattern. Laser sources are much brighter than LEDs.

Laser action is the result of three key processes. These are photon absorption, spontaneous emission and stimulated emission. These three processes are represented by the simple two energy-level diagram in fig., where E_1 is the ground-state energy and E_2 is the excited state energy. According to Planck’s law, a transition between these two states involves the absorption or emission of a photon energy $h\nu_{12}=E_2-E_1$. Normally the system is in the ground state. When a photon of energy $h\nu_{12}$ impinges on the system, an electron in state E_1 can absorb the photon energy and be excited to state E_2 and is called absorption. Since this is an unstable state, the electron will shortly return to the ground state, thereby emitting a photon of energy $h\nu_{12}$. This occurs without any external stimulation and is called spontaneous. The emissions are isotropic and of random phase and, thus, appear as a narrowband Gaussian output. When a photon of energy $h\nu_{12}$ impinges on the system while the electron is in excited state, the electron is immediately

stimulated to drop to the ground state and give off a photon of energy $h\nu_{12}$. This is in phase with the incident photon and the resultant emission is known as stimulated emission.

In thermal equilibrium, the density of excited electrons is very small. Most photons incident on the system will, therefore, be absorbed, so that stimulated emission is essentially negligible. Stimulated emission will exceed absorption only if the population of excited states is greater than that of ground state. The condition is called population inversion. Since this is not an equilibrium condition, population inversion is achieved by various "pumping" techniques. In a semiconductor laser, population inversion is accomplished by injecting electrons into the material at the device contacts to fill the lower energy states of the conduction band. In solid state lasers like the ruby laser or Neodymium laser, light from a powerful source is absorbed in the active medium and increases the population of a number of higher energy levels. In gas lasers a similar metastable level is preferentially populated with the help of electronic excitation.

2.5.2 Optical detectors

An optical detector is a photon (Light) to electron converter. Avalanche photo-diode (APD) and positive intrinsic negative (PIN) diode are most commonly used detectors. The most important thing of the optical communication system is that the spectral response of both the source and the detector must be same, otherwise efficiency will suffer.

2.5.2.1 PIN diode

PIN is the simplest optical detector. It is composed of an n^+ substrate, a lightly doped intrinsic region and a thin p zone. Operated with a reverse bias, mobile carriers level the p-n junction producing a zone of moderate electric field on both sides of the junction into the intrinsic region. As it is only lightly doped, this field extends deeply. Incident light power is mainly absorbed in the intrinsic region, causing electron hole pairs to be generated. These carriers are separated by the influence of the electric field in the intrinsic region and represent a reverse diode current that can be amplified.

2.5.2.2 Avalanche Photo Diode (APD)

It is second popular type of photo detector and has the advantage of internally multiplying the primary detected photocurrent by avalanche process, thus increasing the signal detection sensitivity[27]. But some noises are also generated here. The frequency response of both PIN and APD are similar, making them both suitable up to 1 GHz. The main advantage of APD over PIN diode is greater gain bandwidth product due to the inbuilt gain. Silica is the material used at short wavelength ($< 1\text{nm}$), GE, InGaAsP and AlGaAsP becoming popular at the longer wavelength around $1.3\ \mu\text{m}$.

2.4 IM/DD Channels

Modulation technique for radio wireless system include amplitude, phase and frequency modulation (AM, PM, and FM) as well as some generalizations of these techniques. Radio receivers employ one or more antennas, each followed by a heterodyne of homodyne down-converter, which is comprised of a local oscillator and a mixer. Efficient operation of this relies upon the fact that it receives both the carrier and the local oscillator in a common electromagnetic mode. The down-converter output is an electrical signal whose voltage is linear in the amplitude of the received carrier electric field.

In a low cost optical wireless system, it is extremely difficult to collect appreciable signal power in a single electromagnetic mode. This spatiality incoherent reception makes it difficult to construct an efficient heterodyne or homodyne down-converter for AM, PM, and FM, or to detect AM or PM by any other means. For optical wireless links, the most viable modulation is intensity modulation (IM), in which the desired waveform is modulated onto the instantaneous power of the carrier[21-26]. The most practical down-conversion technique is direct detection (DD), in which a photo detector produces a

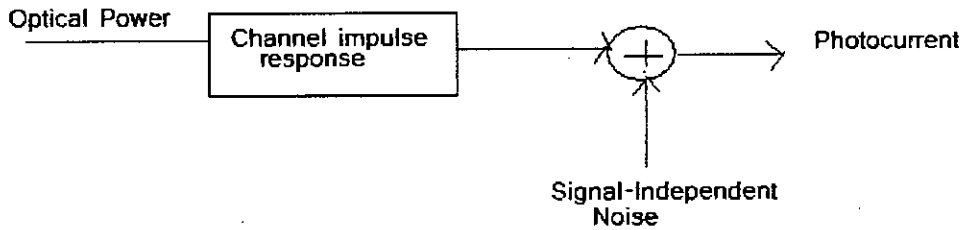


Fig.2.3 Modeling Link as a baseband filter, time-invariant system having impulse response $h(t)$, with signal-independent, additive noise $N(t)$. The photodetector has responsivity R

current proportional to the received instantaneous power, i.e., proportional to the square of the received electrical field.

The modeling of optical wireless channels with IM/DD is illustrated in Fig.2.3. The transmitted waveform $X(t)$ is the instantaneous optical power of the lightwave emitter. The received waveform $Y(t)$ is the instantaneous current in the receiving photo detector which is proportional to the integral over the photo detector surface of the total instantaneous optical power at each location. The received electric field generally displays spatial variation of magnitude and phase, so that a multi-path fading would be experienced if the detector were smaller than a wavelength. Fortunately, typical detector areas are millions of square wavelength, leading to spatial diversity that prevents a multi-path fading. Thus when the detector is moved by a distance of the order of wavelength, no change in the channel is observed. As the transmitted optical power $X(t)$ propagates along various paths of different lengths, optical wireless channels are still subject to multi-path distortion. This distortion is most pronounced in links utilizing non-directional transmitters and receivers, and especially when non-LOS propagation is employed. The channel can be modeled as a baseband linear system, with instantaneous input power $X(t)$, output current $Y(t)$, and an impulse response $h(t)$, as shown in Fig.2.2. Alternatively, the channel can be described in terms of the frequency response

$$H(f) = \int_{-\infty}^{\infty} h(t)e^{-j2\pi ft} dt \quad 2.1$$

Where $H(f)$ is the Fourier transform of $h(t)$. It is usually appropriate to model the channel $h(t)$ $H(f)$ as fixed, since it usually changes only when the transmitter, receiver or objects in the room are moved by tens of centimeters. The linear relationship between $X(t)$ and $Y(t)$

is a consequence of the fact that the received signal consists of many electromagnetic modes. By contrast, we note that when IM/DD is employed in dispersive single-mode optical fiber, the relationship between $X(t)$ and $Y(t)$ is sometimes nonlinear. In many applications, optical wireless links are operated in the presence of intense infrared and visible background light. While received background light can be minimized by optical filtering, it still adds shot noise, which is usually the limiting noise source in a well designed receiver. Due to its high intensity, this shot noise can be modeled as additive, white, Gaussian and independent of $X(t)$. When little or no ambient light is present, the dominant noise source is receiver preamplifier noise, which is also signal-independent and Gaussian (though often non-white). Thus we usually model the noise $N(t)$ as Gaussian and signal-independent. This stands in contrast to the signal-independent, Poisson noise considered in photon-counting channel models. Fluorescent lamps emit infrared that is modulated in nearly periodic fashion, when present; this adds a cyclostationary component to $N(t)$ [75-76].

The baseband channel model is summarized by

$$Y(t) = R X(t) \otimes h(t) + N(t) \quad 2.2$$

Where the symbol \otimes denotes convolution and R is the detector responsivity (A/W). While Eq.(2.2) is simply a conventional linear filter channel with additive noise, optical wireless systems differ from conventional electrical or radio systems in several respects. Because the channel input $X(t)$ represents instantaneous optical power, the channel input is non-negative;

$$X(t) \geq 0 \quad 2.3$$

And the average transmitted optical power P_t is given by

$$P_t = \lim_{T \rightarrow \infty} \frac{1}{2T} \int_{-T}^T X(t) dt \quad 2.4$$

Rather than the usual time-average of $|X(t)|^2$ which is appropriate when $X(t)$ represents amplitude. The average received optical power is given by

$$P = H(0) P_t \quad 2.5$$

Where the channel d.c. gain is $H(0) = \int_{-\infty}^{\infty} h(t) dt$. The performance of a wireless optical link at bit rate R_b is related to the received electrical SNR

$$\text{SNR} = \frac{R^2 P^2}{R_b N_0} = \frac{R^2 H^2(0) R^2 P^2}{R_b N_0} \quad 2.6$$

Assuming that $N(t)$ is dominated by a Gaussian component having double-sided power spectral density N_0 from Eq. (2.6), we see that SNR depends on the square of the received optical average power, implying that IM/DD optical wireless links must transmit at a relatively high power and can tolerate only a limited path loss. This stands in contrast to the case of radio wave channels, where the SNR is proportional to the first power of the received average power.

2.5 Design of Power Efficient Links

Achieving a high electrical SNR is the single biggest problem facing the designer of an optical wireless link. The difficulty arises for two reasons. Firstly, the SNR of an IM/DD link depends upon the square of the received optical average power. This implies that one should transmit at relatively high power, but available transmitter power may be limited by considerations of eye safety and power consumption. It also implies that one should design the link so as to minimize path loss and employ a receiver having a large light-collection area. Second, in many environments there exists intense ambient infrared noise, which introduces white shot noise and low-frequency cyclostationary noise into the receiver. This noise can be minimized through optical filtering and by employing a directional receiver, which can separate the desired signal from the ambient noise.

2.6 Optical Transmitter and Eye safety

The wavelength band between approximately 780 and 950 nm is presently the best choice for the most present applications of optical wireless links, due to the availability of low cost LEDs and laser diode (LDs) and because it coincides with the peak responsivity of inexpensive, low-capacitance silicon photo diodes. The primary drawback of radiation in this band relates to eye safety i.e. it can pass through human cornea and be focused by the

lens onto the retina, where it can potentially induce thermal damage. The cornea is opaque to radiation at wavelength beyond approximately 1400 nm, considerably reducing potential ocular hazard, so that it has been suggested that the 1550 nm band may be better suited for optical wireless links. Unfortunately, the photo diodes presently available for this band, which are made of germanium or InGaAs, have much higher costs and capacitances per unit area than their silicon counterparts. To our knowledge, at present all commercially available systems operate in the shorter-wavelength band.

Table 2.2 presents a comparison between LEDs and LDs. LEDs are currently used in all indoor commercial systems, due to their extremely low cost and because most LEDs emit light from a sufficiently large surface area that they are generally considered eye-safe. Typical packaged LEDs emit light into semi-angle (at half power) ranging from approximately 10-30 degrees, making them suitable for directed transmitters. Non-directed transmitter's frequency employ multiple LED's oriented in different directions.

Table 2.2: Comparison between LED's and LD's

Characteristics	LED	LD
Spectral Width	25-100 nm (10-50 THz)	$<10^{-5}$ to 5 nm (<1 MHz to 2 THz)
Modulation Bandwidth	Tens of KHz to tens of MHz	Tens of KHz to tens of GHz
E/O Conversion Efficiency	10-20%	30-70%
Eye Safety	Generally considered eye safety	Must be rendered eye-safe, Especially for $\lambda < 1400$ nm
Cost	Low	Moderate to high

Potential drawbacks of present LED's include:

- 1) Typically poor electro-optic power conversion efficiencies of 10-20 % (though new devices have efficiencies as high as 40%)
- 2) Modulation band width that are limited to tens of MHZ in typical low cost devices
- 3) Broad spectral width (typically 25-100 nm), which require the use of a wide receiver optical pass band, leading to poor rejection of ambient light and
- 4) The fact that wide modulation bandwidth is usually obtained at the expense of reduced electro-optic conversion efficiency.

LD's are much expensive than LED's, but offer many nearly ideal characteristics:

- 1) Electro-optic conversion efficiencies of 30-70%.
- 2) Wide modulation bandwidths, which range from hundreds of MHZ to more than 10 GHz and
- 3) Very narrow spectral widths (spectral widths ranging from several nm to well below 1 nm are available).

To achieve eye safety with an LD requires that one pass the laser output through some element that destroy its spatial coherence and spreads the radition over a sufficiently extended emission aperture and emission angle. For example, one can employ a transmissive diffuser, such as a thin plate of translucent plastic. While such diffusers can achieve efficiencies of approximately 70%, they typically yield a Lambertian radiation pattern, offering the designer little freedom to tailor the source radiation pattern. Computer-generated holograms offer a means to generate custom-tailored radiation patterns with efficiencies approaching 100%, but must be fabricated with care to insure that any residual image of the LD emission aperture is tolerably weak.

Recently, RCLEDs (Resonant Cavity LEDs) have been developed. Their structure are epitaxially grown by MBE on double polished n^+ GaAs substrates and emit through the substrates and emit through the substrate, which is nominally transparent at these wavelengths. The active layers in the cavity are 3 or 4 strained $\text{In}_x\text{Ga}_{1-x}\text{As}$ ($x \sim 0.17$) Quantum wells (QWs) clad by GaAs barrier layers. The bottom mirror is a multiple quarter-GaAs/AlAs layers, known as a Distributed Bragg Reflector (DBR). The cavity is completed by the deposition of a metal mirror on the upper surface of the multilayer structure. A key property of RCLEDs of application is the ability to determine the emission angular beam profile by designing the emission wavelength of the QWs inside the cavity to be approximately 10-20 nm shorter than the resonance wavelength of the cavity. Moreover the modulation bandwidth of RCLEDs is achieved to approximately 500 MHz.

The eye safety of infrared transmitters is governed by International Electro-technical Commission (IEC) standards [3]. It is desirable for infrared transmitters to conform to the IEC Class 1 allowable exposure limit (AEL), implying that they are safe under all foreseen circumstances of use, and require no warning labels. At pulse repetition rates higher than 24 KHz, compliance with this AEL can be calculated on the basis of average emitted optical power alone. The AEL depends on the wavelength, diameter, and emission semiangle to the source. At present, the IEC is in midst of revising the standards applying to infrared transmitters. Based on proposed revisions, at 875 nm, an IrDA-compliant source having an emission semiangle of 15 degrees and diameter of 1 mm can emit up to 280 mW, at larger diameters, the allowable power increases is the square of the diamete

Chapter 3

Analysis of Optical Code Division Multiple Access (OCDMA) Transmission System

3.1 The principle of spread spectrum

In spread techniques, a modulated signal is further modulated (spread) by a noise-like code of much higher bit rate in such a way as to generate an extended bandwidth signal that does not significantly interfere with other signals and resembles white noise. Bandwidth expansion is achieved by a second modulation means. The receiver can only detect the signal and extract it from noisy signal if its knows the spreading code (signature sequence) that has been used to spread the signal[28-34].

The term spread spectrum has been used in a wide variety of military and commercial communication system. In spread spectrum systems each information signal requires significantly more radio frequency (RF) bandwidth than a conventional modulated signal would require. The benefits of using spread spectrum techniques are:

1. Improved interference rejection
2. Code division multiplexing for code division multiple access (CDMA) application.
3. Low density power spectra for signal hiding.
4. High resolution ranging.
5. Secured communication.
6. Lower cost of implementation readily available IC(Integrated Circuit)components.

3.2 Radio frequency communications spread spectrum techniques

The most commonly employed spread spectrum modulations techniques in electrical domains are:

1. Direct sequence spread spectrum (DS-SS), including CDMA.
2. Frequency hopped (FH) spread spectrum, including slow frequency hopping (SFH) and fast frequency hopping (FFH) system.
3. Carrier sense multiple access (CSMA) spread spectrum.
4. Time hopping.
5. Hybrid Spread Spectrum Method.

In more radio systems and wireless local area networks (WLAN), direct sequence, frequency-hopped CDMA, and methods have been extensively used. Brief description of direct sequence and frequency hopped spread spectrum techniques is given below.

3.2.1 Direct sequence spread spectrum

Direct sequence CDMA is automatically associated to a spread spectrum communication system [30]. The message is first modulated by traditional amplitude, frequency or phase techniques. A pseudo noise signal is then used as a code sequence (PN code) to spread the modulated waveform over a relative wide bandwidth. The signal message may be also coded by the code sequences and after that, modulated by a BPSK (for example) waveform. A schematic block diagram of direct-sequence spread spectrum system is given in Figs.3.1(a) and 3.2(b). The digital binary base-band information, $d(t)$, also known as nonreturn zero(NRZ) data, having a source bit rate of $R_b=1/T_b$, modulated by BPSK (for example) in the first modulator. $d(t)$ is an unfiltered binary signal having two states +1 or -1. The direct sequence spread spectrum may be obtained by multiplying the modulated signal $S(t)$ by a pseudorandom noise signal $g(t)$ having a chip rate of $R_c=1/T_c$.

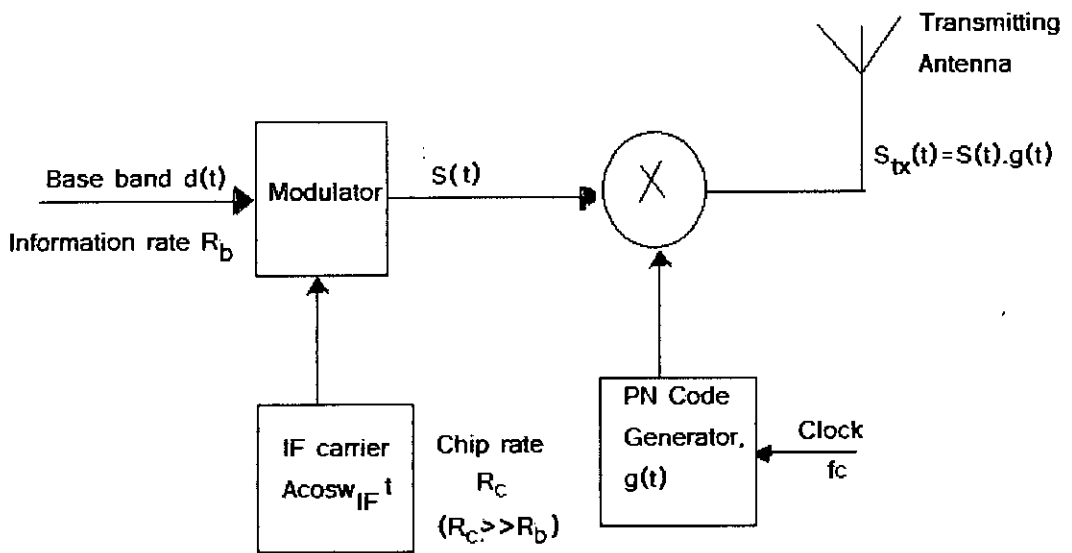


Fig 3.1(a) Direct Sequence spread Spectrum Block Diagram (Transmitter)

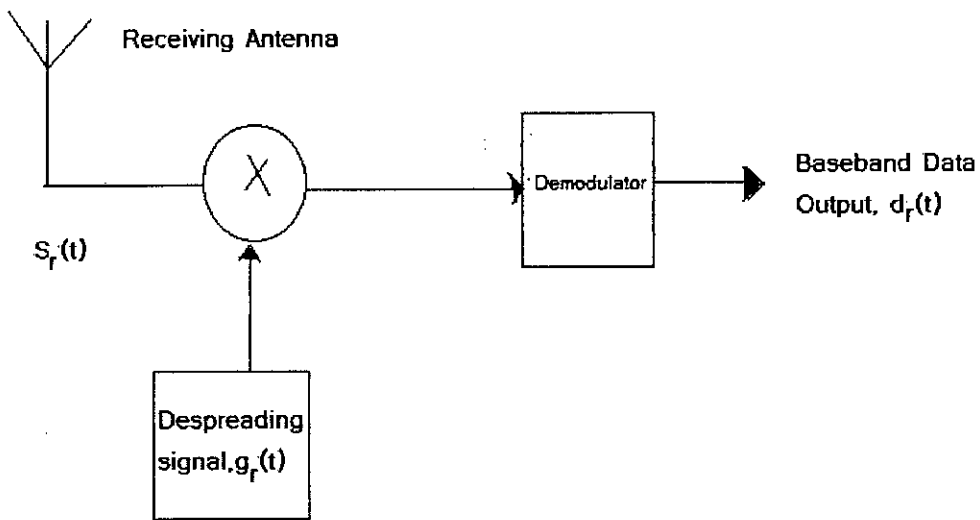


Fig 3.1(b) Direct Sequence spread Spectrum Block Diagram (Receiver)

Transmitted signal can be written as

$$S_{tx}(t) = S(t) \cdot g(t) \quad (3.1)$$

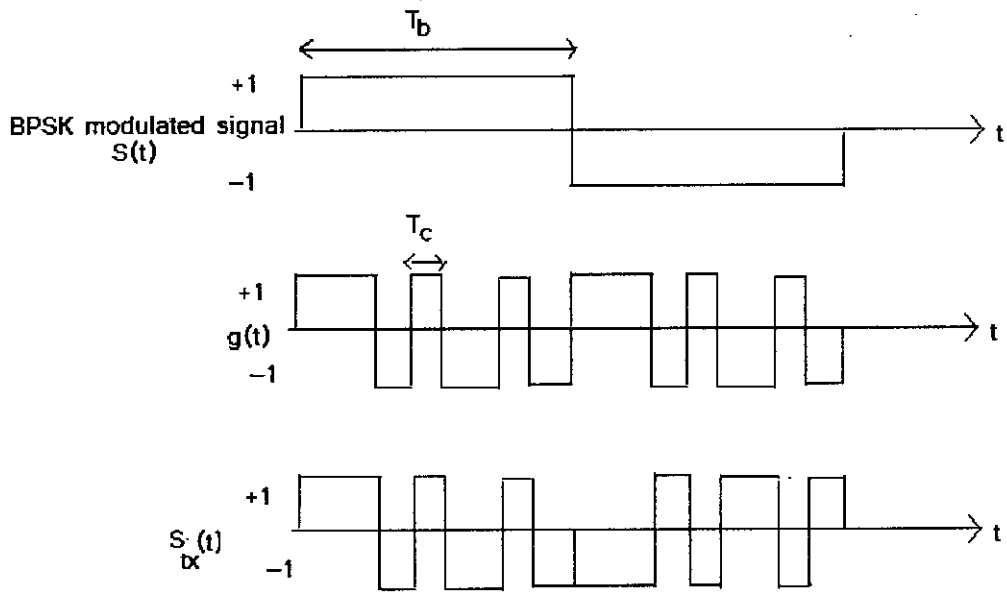


Fig.3.2 Spread spectrum modulation in time domain

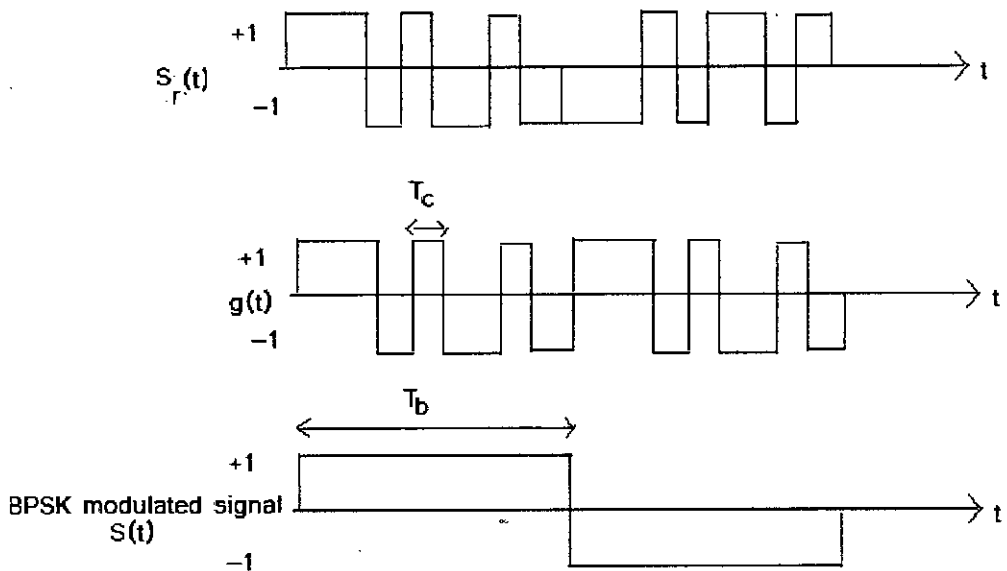


Fig.3.3 Spread spectrum demodulation in time domain

Fig.3.2 gives an example of this modulation in time domain. The effect of multiplication of BPSK modulated signal with PN sequence $g(t)$ is to spread the bandwidth R_b of $S(t)$ to a bandwidth of R_c . The spread spectrum signal can not be detected by a conventional narrow band receiver.

In the receiver, the received signal $S_r(t)$ is multiplied with the PN signal $g_r(t)$. If $g_r(t)=g(t)$ and synchronized to the PN sequence in the received data, then the recovered binary data is produced on $d_r(t)$. The spread spectrum demodulation is shown in fig. 3.3 in time domain. The effect of multiplication of the spread spectrum signal $S_r(t)$ with the PN sequence $g(t)$ used in the transmitter is to disperse the bandwidth of $S_r(t)$ to R_b . If $g_r(t)\neq g(t)$, then there is no despreading action. The signal $d_r(t)$ is spread spectrum, thus, a receiver not knowing the PN sequence of transmitter can not reproduce the transmitter data.

3.2.2 Frequency hopped spread spectrum

In frequency hopping spread spectrum, the chips, that compose the code sequence assigned to a given user, are modulated in frequency. Each of the N chips corresponds to a sinusoidal waveform whose frequency is chosen pseudo-randomly from a given set of frequencies. In addition to the appropriate codewords choices, the frequency hopping model may be reduce the multi access interference created by the users messages. Frequency hopping model is considered as slow when several data bits are transmitted at the same frequency. In opposite, frequency hopping model is considered as fast when the chips, in one bit, are transmitted at different frequencies.

3.3 Spread spectrum as a multiple access techniques

There are a number of spread spectrum techniques, depending on the domain in which the signal space is shared among the remote users:

FDMA-frequency division multiple access

CDMA-code division multiple access

TDMA-time division multiple access

SDMA-space division multiple access

PDMA-polarization division multiple access

In FDMA each user gets allocated a frequency channel for its sole use, in TDMA it is a time slot in time frame. In CDMA all users transmit in the same frequency band for all time, but they are separated by the codes allocated to them. The last two multiple access techniques are used on their own, but combination with the first three to enhance the system capacity.

The advantage of CDMA for personal communication services is its ability to accommodate many users on the same frequency at the same time. As we mentioned earlier, a specific code is assigned to each user and only that code can demodulate the transmitted signal, multiple access in CDMA can be two ways:

Orthogonal Multiple Access

Non-orthogonal Multiple Access or Asynchronous CDMA

3.4 Orthogonal Multiple Access

Orthogonal multiple access is used in synchronous CDMA in which user is assigned one or many orthogonal waveform derived from an orthogonal-code[35-36]. Since the waveforms are orthogonal, user with different codes do not interfere with each other.

3.4.1 Orthogonal Codes

Walsh set is one of the most important set of orthogonal code. Walsh functions are generated using an iterative process of constructing a Hadamard matrix starting with $H_1 = [0]$. The Hadamard matrix is built by:

$$H_{2n} = \begin{pmatrix} H_n & H_n \\ H_n & H_n \end{pmatrix}$$

Walsh-Hadamard codes of length 2 and 4 are given below.

$$H_2 = \begin{pmatrix} 0 & 0 \\ 0 & 1 \end{pmatrix}$$

$$H_4 = \begin{pmatrix} 0 & 0 & 0 & 0 \\ 0 & 1 & 0 & 1 \\ 0 & 0 & 1 & 1 \\ 0 & 1 & 1 & 0 \end{pmatrix}$$

From the corresponding matrix, the Walsh-Hadamard codewords are given by the rows, polar form can be achieved from the binary data of Walsh-Hadamard codewords mapping 0's to 1's to -1.

Walsh-Hadamard codes are orthogonal codes with different codes with different spreading factors. This property becomes useful when we want signals with different spreading factors to share the same frequency channel[40-44]. However, the auto-correlation

Characteristics of Walsh-Hadamard codewords is not good one because it can have more than one peak. Thus, it is not possible for the receiver to detect the beginning of the

codeword without an external synchronization scheme. Power spectral density of Walsh-Hadamard codes is concentrated in a small number of discrete frequencies and cross-correlation can also be non zero for a number of time shifts. Thus, Walsh-Hadamard codes do not have the best spreading behavior and un-synchronized users can interfere with each other. This is why Walsh-Hadamard codes can not be used in asynchronous CDMA[32-33].

3.5 Non-orthogonal Multiple Access

Non-orthogonal multiple access is used in asynchronous CDMA. The code sequences which have good spreading behavior, balance property, higher number of independent sequence, autocorrelation and cross-correlation property is used for asynchronous CDMA [37-39]. PN sequences are used to spread the spectrum. Gold sequence and m-sequence are in the family of PN sequence but Gold sequence is in particular popular for non-orthogonal CDMA.

3.5.1 m-Sequence

Maximal length shift register sequence are still of importance in digital communications and in spread spectrum and ranging systems. The widely used hardware implementation of a PN sequence generator and corresponding correlator and matched data filter register has been shown in Fig.3.4. The generator contains type D flip flops and is connected so that each data input except D_0 is the Q output of the preceding flip flop. Not all Q flip flop outputs need be connected to the parity generator (indicated by dashed lines). The number of flip flops n and the selection of which flip flop outputs are connected to the parity generator determine the length and the characteristics of the generated PN sequence.

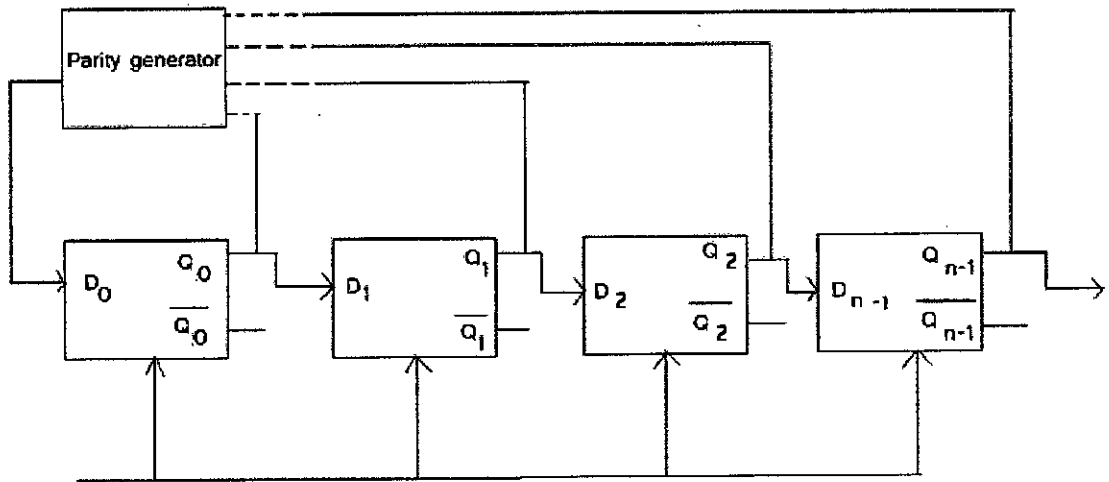


Fig.3.4 Hardware of a pseudo-noise (PN) generator

The parity generator provides an output logic 0, when an even number of inputs are at logic 0 and generates logic 1 output when an odd number of inputs are at logic 1 state.

3.5.1.1 Properties of m-sequence:

Balance property

In each period of the sequence, the number of binary ones differs from the number of binary zeros by one digit. In m-sequence number of ones is 2^{n-1} and number of zeros is $2^{n-1}-1$ where n is number of flip-flops. For example, 1110010 is a 7 chip m-sequence in which number of ones is 4 and number of zeros is 3.

$$\sum g(t) = \sum 1+1+1-1-1+1-1=1$$

When modulating a carrier with a m-sequence, one-zero balance (DC components) can limit the degree of carrier suppression obtainable, because carrier suppression is dependent on the symmetry of the modulating signal.

Sequence Length

For maximal length linear codes, it is always possible to find a set of connections from flip-flop outputs to the parity generator that will yield a maximal length sequence of

$$L=2^n-1 \quad (3.2)$$

Where n is the number of flip flops. A specific connection diagram of flip flop outputs to the parity generator input illustrated in Table 3.1.

Table 3.1 Numerical values of flip flop outputs to the parity generator input are illustrated in table

Number of Stages n	Sequence length $L=2^n-1$	S= Number of m Sequence	Do for $L=2^n-1$ in fig. 5.5
3	7	2	$Q_1 \otimes Q_2$
4	15	2	$Q_2 \otimes Q_3$
5	31	6	$Q_2 \otimes Q_4$
6	63	6	$Q_4 \otimes Q_5$
7	127	18	$Q_5 \otimes Q_6$
8	255	16	$Q_1 \otimes Q_2 \otimes Q_3 \otimes Q_7$
9	511	48	$Q_4 \otimes Q_8$
10	1023	60	$Q_6 \otimes Q_9$
11	2047	176	$Q_8 \otimes Q_{10}$
12	4095	144	$Q_1 \otimes Q_9 \otimes Q_{10} \otimes Q_{11}$
13	8191	630	$Q_0 \otimes Q_{10} \otimes Q_{11} \otimes Q_{12}$
14	16383	756	$Q_1 \otimes Q_{11} \otimes Q_{12} \otimes Q_{13}$
15	32767	1800	$Q_{13} \otimes Q_{14}$

The resultant maximal-length PN sequence L is between 7 & 32767 bits.

Impedence Sequence:

One possible logic design connection is illustrated in Table 3.1. There are many possible connections the parity generator, which has correlation with one another. The upper bound S of the number of independent sequence is given by

$$S \leq \frac{L-1}{n} \quad (3.3)$$

Autocorrelation Property:

The m-sequences have an interesting cyclic or periodic autocorrelation property. The origin of the name pseudo noise is that it has an autocorrelation function very similar to that of white noise signal [45]. The auto correlation of m-sequence is -1 for all values of chip phase shift τ , except for the [-1, +1] chip phase shift area, in which correlation varies linearly from the -1 value to $L = 2^n - 1$ (the sequence length). Replacing each 0 by -1 and each 1 by +1, then the periodic correlation function is given by

$$R(\tau) = \begin{cases} 2^n - 1, & \tau = 0 \\ -1, & \tau \neq 0 \end{cases} \quad (3.4)$$

For an $n=3$ stage shift register generator, generating a 7 bit maximal length pseudorandom code, with a chip rate of 10Mc/s and a 7 bit reference sequence 1110010, Time domain agreements (A) and disagreement (D) for shift $\tau=0$ but $A=3$ and $D=4$ for $\tau=1$. The table of the number of agreements (A) and disagreement (D) by lining up the shifted autocorrelation code sequence in one bit increment is given in table 3.2. Auto-correlation function is shown in Fig.3.5.

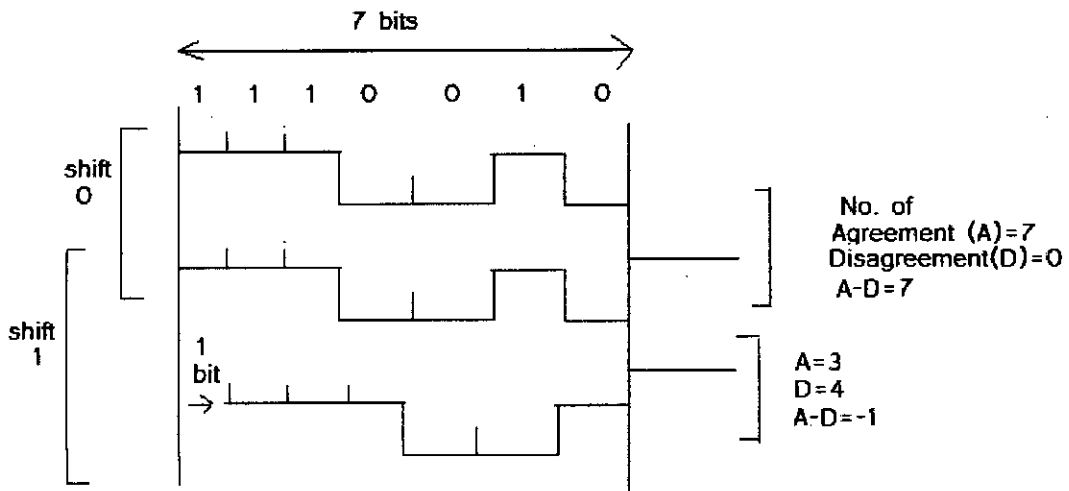


Fig. 3.5 Auto correlation of 7 chip m-sequence with shift 1

Table 3.2 Reference Sequence: 1110010

Shift	Sequence	Agreements(A)	Disagreements(D)	A-D
0	1110010	7	0	7
1	0111001	3	4	-1
2	1011100	3	4	-1
3	0101110	3	4	-1
4	0010111	3	4	-1
5	1001011	3	4	-1
6	1100101	3	4	-1

Cross-correlation property

Cross-correlation is the measure of between two different two different codes. This property is very important for asynchronous CDMA because multiple access interference (MAI) depends on this property [46]. Unfortunately, cross-correlation is not so well behaved as auto-correlation. When large numbers of transmitters, using different codes, are to share a common frequency band, the code sequence must be carefully chosen to avoid interference among users.

3.5.2 Gold Sequence

In contrast to simple m-sequence, Gold-sequences are suitable for multiple user CDMA systems. They offer a large number of sequences sets with good cross-correlation properties between the single sequences. Gold sequences have only three cross-correlation peaks, which tend to get less important as the length of the code increases. They also have a single auto-correlation peak at zero, just like ordinary PN sequences.

The gold sequences are generated by modulo-2 addition of two m-sequences of same length clocked by the same chip-clock (Fig.3.6). Since both m-sequences have equal length L and use the same clock, the created the gold sequence is of length L and use the

same clock. If n is the number of stages in each m-sequence generator then the length of generated Gold sequence $L = 2^{n-1} - 1$

It can be shown that for any shift in the initial conditions between the two m-sequences a new gold sequence is generated.

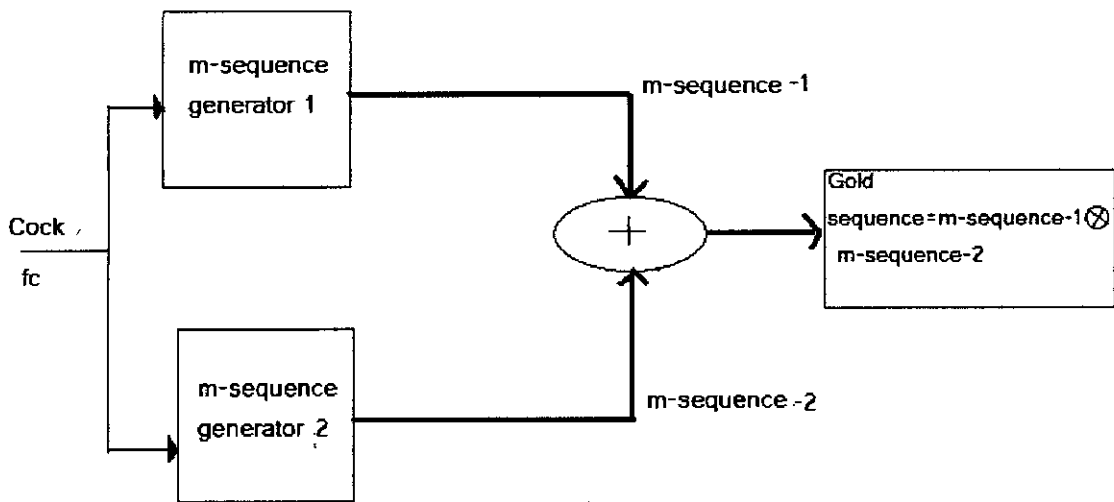


Fig. 3.6 Block diagram of Gold Sequence Generator

Thus a gold sequence generator combining two different m sequence can create a number of different $L = 2^{n-1} - 1$ Gold sequences. But all of them have no good cross-correlation property. The m-sequences pair which gives only three cross-correlation peaks is used to generate Gold-sequence.

3.5.3 Prime code

Prime codes are a family of optical address codes that are suitable for optical fiber code-division multiple access (CDMA) systems using all-optical processing. However, the code weight w of a prime code is always fixed to the maximum number of users N . This means that, once N becomes large (e.g. in a system with many users), the resulting cost and optical power losses of all-optical CDMA encoder/decoder can be high. In turn, this may prevent the use of integrated optics from implementing such encoders and decoders. To effectively solve these problems, we present the partial modified prime (PMP) codes for all-optical CDMA systems. It is shown that PMP codes can maintain the fixed w for a given bit error rate (e.g. 10^{-9}) but for any N . We also prove that PMP codes preserve the same cross-correlation constraint as original prime codes. So far, prime codes and optical orthogonal codes (OOCs) have been widely studied for OCDMA applications [46-50]. It is known that OOCs have better properties of auto- and cross-correlation than prime codes. However, much more complex algorithms are required to generate and correlate the OOCs [52] than the prime codes. Since the generation of prime codes is extremely simple (i.e. based on modulo-multiplications)[51], this in turn can greatly reduce the processing time in an OCDMA system to guarantee real-time high-speed data communications. Moreover, a prime code can be divided into P equal-length subsequences of which each contains only one pulse, where P is a prime number. Consequently, these characteristics make prime codes very adequate for OCDMA systems that use a single optical tunable delay line as an encoder to achieve a fast reconfiguration time at each transmitter [57]. However, a major problem associated with prime codes is that their code weight w is always fixed to the number of code words (i.e. code size) and must be a prime number p [51]. To accommodate more users in an OCDMA system, a larger P is required, so is the code weight w . Since all-optical CDMA encoders and decoders for prime codes use a 'parallel' configuration, the resulting optical power losses and complexity of an encoder or decoder would be high if w becomes large. For example, the power loss of an all-parallel encoder (or decoder) is as high as 35.4 dB

if $p = 59$, and the required number of optical delay lines per encoder (or decoder) is equal to $w = p = 59$. In this case, the encoders and decoders are also bulky, which may prevent their implementation by using integrated optics. As reported in [51-54], the bit error rate (BER) of incoherent OCDMA systems using a prime code is decreased with increasing w . When P is large enough (e.g., $P \geq 41$ for OCDMA systems without optical hard-limiting), the BER becomes very low even if all the users simultaneously transmit data in the system. Thus, it is expected that we can choose a lower w than that of the large-weight prime code to ensure a prescribed BER (e.g. 10^{-9}) by removing some 'redundant' pulses from the original prime code of P pulses. This results in the construction of the modified prime (PMP) codes for OCDMA applications. Subsequently, we will prove that PMP codes still preserve the same cross-correlation constraint as original prime codes. Then we will show how to reasonably choose the weight and length of PMP codes for OCDMA systems to optimize the system performance.

3.5.3.1 Construction of Partial Modified Prime Codes (PMP)

The prime codes are a set of code sequences with code length $L = p^2$ derived from prime sequences, where p is a prime number [51]. Elements of a prime sequence can be obtained by multiplying each element in the Galois field $GF(p) = \{0, 1, \dots, (p-1)\}$ by a preset number chosen from $GF(p)$. Hence, there are p prime sequences. We then map these prime sequences to binary code sequences to form the prime codes. For example, the prime sequence $S_x = (S_{x,0}, S_{x,1}, \dots, S_{x,i}, \dots, S_{x,(p-1)})$ is mapped to the code sequence $C_x = (C_{x,0}, C_{x,1}, \dots, C_{x,i}, \dots, C_{x,(p^2-1)})$ according to

$$C_{x,i} = \begin{cases} 1 & \text{for } i = S_{x,j} + jp, \quad j = 0, 1, \dots, p-1 \\ 0 & \text{otherwise} \end{cases} \quad (3.5)$$

On the other hand, the modified prime codes, which are used in synchronous systems, are time-shift versions of the prime codes [54]. To construct the modified prime codes, we take a prime sequence S_x and rotate it by $(p-1)$ times to create new prime sequences $S_{x,r} = (S_{x,r,0}, S_{x,r,1}, \dots, S_{x,r,i}, \dots, S_{x,r,(p-1)})$, where r refers to the number of left-rotations. Likewise, the mapped code sequence $C_{x,r} = (C_{x,r,0}, C_{x,r,1}, \dots, C_{x,r,i}, \dots, C_{x,r,(p^2-1)})$ can be obtained according to

$$C_{x,r,i} = \begin{cases} 1 & \text{for } i = S_{x,r,j} + jp, \quad j = 0,1,\dots,p-1 \\ 0 & \text{otherwise} \end{cases} \quad (3.6)$$

Each prime code sequence can generate $p-1$ new code sequences to form a code group. Hence, the modified prime codes can be divided into p groups and the total number of codes is p^2 . An example of the modified prime codes derived from is GF (5) is shown in Table 3.3. Under synchronized condition, the cross-correlation between the x th and y th modified prime codes is

$$\Gamma_{x,y} = \begin{cases} p, & x = y \\ 0, & x \text{ and } y \text{ are in the same group} \\ 1, & x \text{ and } y \text{ are in different groups} \end{cases} \quad (3.7)$$

TABLE 3.3
Example of the Modified Prime Codes for GF (5)

Group x	i	Sequence	Code Sequence
	01234		
0	00000	$S_{0,0}$	$C_{0,0} = 10000 \quad 10000 \quad 10000 \quad 10000 \quad 10000$
	44444	$S_{0,1}$	$C_{0,1} = 00001 \quad 00001 \quad 00001 \quad 00001 \quad 00001$
	33333	$S_{0,2}$	$C_{0,2} = 00010 \quad 00010 \quad 00010 \quad 00010 \quad 00010$
	22222	$S_{0,3}$	$C_{0,3} = 00100 \quad 00100 \quad 00100 \quad 00100 \quad 00100$
	11111	$S_{0,4}$	$C_{0,4} = 01000 \quad 01000 \quad 01000 \quad 01000 \quad 01000$
1	01234	$S_{1,0}$	$C_{1,0} = 10000 \quad 01000 \quad 00100 \quad 00010 \quad 00001$
	12340	$S_{1,1}$	$C_{1,1} = 01000 \quad 00100 \quad 00010 \quad 00001 \quad 01000$
	23401	$S_{1,2}$	$C_{1,2} = 00100 \quad 00010 \quad 00001 \quad 10000 \quad 01000$
	34012	$S_{1,3}$	$C_{1,3} = 00010 \quad 00001 \quad 10000 \quad 01000 \quad 00100$
	40123	$S_{1,4}$	$C_{1,4} = 00001 \quad 10000 \quad 01000 \quad 00200 \quad 00010$
2	02413	$S_{2,0}$	$C_{2,0} = 10000 \quad 00100 \quad 00001 \quad 01000 \quad 00010$
	24130	$S_{2,1}$	$C_{2,1} = 00100 \quad 00001 \quad 01000 \quad 00010 \quad 10000$
	41302	$S_{2,2}$	$C_{2,2} = 00001 \quad 01000 \quad 00010 \quad 10000 \quad 00100$
	13024	$S_{2,3}$	$C_{2,3} = 01000 \quad 00010 \quad 10000 \quad 00100 \quad 00001$
	30241	$S_{2,4}$	$C_{2,4} = 00010 \quad 10000 \quad 00100 \quad 00001 \quad 01000$
3	03142	$S_{3,0}$	$C_{3,0} = 10000 \quad 00010 \quad 01000 \quad 00001 \quad 00100$
	31420	$S_{3,1}$	$C_{3,1} = 00010 \quad 01000 \quad 00001 \quad 00100 \quad 10000$
	14203	$S_{3,2}$	$C_{3,2} = 01000 \quad 00001 \quad 00100 \quad 10000 \quad 00010$
	42031	$S_{3,3}$	$C_{3,3} = 00001 \quad 00100 \quad 10000 \quad 00010 \quad 01000$
	20314	$S_{3,4}$	$C_{3,4} = 00100 \quad 10000 \quad 00010 \quad 01000 \quad 00001$
4	04321	$S_{4,0}$	$C_{3,0} = 10000 \quad 00001 \quad 00010 \quad 00100 \quad 01000$
	43210	$S_{4,1}$	$C_{3,1} = 00001 \quad 00010 \quad 00100 \quad 01000 \quad 10000$
	32104	$S_{4,2}$	$C_{3,2} = 00010 \quad 00100 \quad 01000 \quad 10000 \quad 00001$
	21043	$S_{4,3}$	$C_{3,3} = 00100 \quad 01000 \quad 10000 \quad 00001 \quad 00010$
	10432	$S_{4,4}$	$C_{3,4} = 01000 \quad 10000 \quad 00001 \quad 00010 \quad 00100$

According to (3.7), the cross-correlation between the x th and y th codes is zero when they belong to the same group or one otherwise. Since the cross-correlation of the modified prime codes is never larger than one, the modified prime codes are superior to the modified quadratic congruence (MQC) codes[71], whose cross-correlation is equal to one, for suppressing PIIN. However, the cross-correlation of the modified prime codes is also equal to one in most situations, i.e., the situation that the codes are in different groups. Hence, the improvement is insignificant.

In order to further suppress the PIIN, we relax the constraint of the cross-correlation of the modified prime codes and propose the PMP codes in this paper to reduce the beating rate between the code sequences. The PMP codes are divided versions of the modified prime codes. Each of the modified prime sequences can be used to generate several new sequences. This means that the modified prime sequence $S_{x,r}$ constructed from GF(p) can be divided to form M new prime sequences $S_{x,r,m}=(S_{x,r,m,0}, S_{x,r,m,1}, \dots, S_{x,r,m,i}, \dots, S_{x,r,m,(p-1)})$, Where M is a factor of $(p-1)$ and $m \in \{0, \dots, M-1\}$.

For instance, if, $M=2$, the modified prime sequence can $S_{x,r}$ can be separated as $S_{x,r,0}=(S_{x,r,0,0}=S_{x,r,0}, S_{x,r,0,1}=X \dots S_{x,r,0,x}=X, \dots S_{x,r,0,(p-2)}=S_{x,r,(p-2)}, S_{x,r,0,(p-1)}=X)$, and $S_{x,r,1}=(S_{x,r,1,0}=X, S_{x,r,1,1}=S_{x,r,1} \dots S_{x,r,1,x}=X, \dots S_{x,r,1,(p-2)}=X, S_{x,r,1,(p-1)}=S_{x,r,(p-1)})$,

Where $X=\text{null}$. The mapped code sequences $C_{x,r,m} = (C_{x,r,m,0}, C_{x,r,m,1}, \dots, C_{x,r,m,i}, \dots, C_{x,r,m,(p-1)})$ can be obtained according to (3.8)

$$C_{x,r,m,i} = \begin{cases} 1 & \text{for } i = S_{x,r,m,j} + jP, \quad j=0,1,\dots,p-1 \text{ and } S_{x,r,m,j} \neq X \\ 0 & \text{otherwise} \end{cases} \quad (3.8)$$

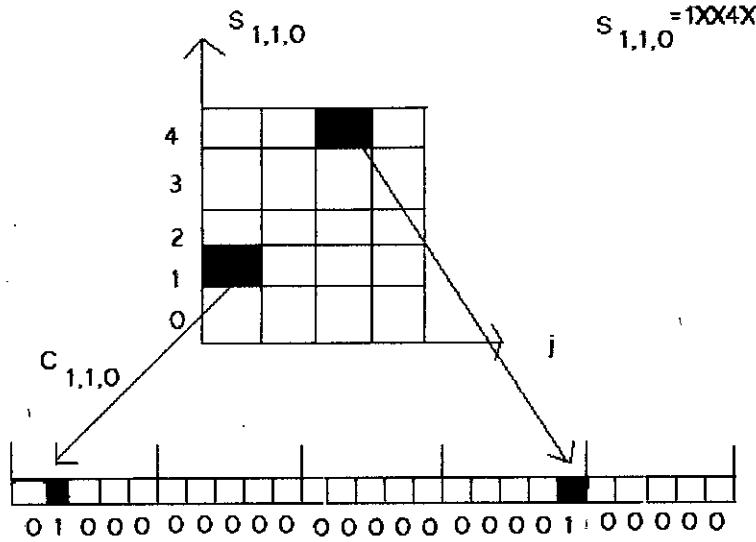


Fig. 3.7 An exemplary procedure for generating (0, 1) sequence $C_{x,r,m}$ based on the partial modified prime sequence $S_{x,r,m}$

By using this scheme, the size of each group of the modified prime codes is expanded M times. The code size of the PMP codes is Mp^2 and the code weight is reduced to $(p-1)/M$. Therefore, the beating rate of any two PMP code sequences can be reduced as the value of the dividing factor M is increased. The PIIN can be further suppressed by optimizing the value of M . An example of the PMP codes for GF (5) and $M=2$ is shown in Table 3.2. Fig.3.7 illustrates an exemplary procedure for generating (0, 1) sequence based on the partial modified prime sequence $S_{x,r,m}$.

Under synchronized condition, the cross-correlation between the x th and y th PMP codes is

$$\Gamma_{x,y} = \begin{cases} (p-1)/M, & x = y \\ 0, & x \text{ and } y \text{ are in the same group} \\ \leq 1, & x \text{ and } y \text{ are in different groups} \end{cases} \quad (3.9)$$

Hence, if $C_m(g)$ denotes the g th element of the n th PMP code sequence, the relation between the code sequences can be written as:

$$\sum_{g=1}^L C_m(g)C_n(g) = \begin{cases} \frac{p-1}{M}, & m = n \\ \leq 1, & m \neq n \end{cases} \quad (3.10)$$

Where L is the code length, i.e. $L=p^2$

TABLE 3.4
Example of the Partial Modified Prime Codes for GF (5) and M=2

Group x	i 01234	Sequence	Code Sequence				
0	X0X0X	$S_{0,0,0}$	$C_{0,0,0} = 00000$	10000	00000	10000	00000
	X4X4X	$S_{0,1,0}$	$C_{0,1,0} = 00000$	00001	00000	00001	00000
	X3X3X	$S_{0,2,0}$	$C_{0,2,0} = 00000$	00010	00000	00010	00000
	X2X2X	$S_{0,3,0}$	$C_{0,3,0} = 00000$	00100	00000	00100	00000
	X1X1X	$S_{0,4,0}$	$C_{0,4,0} = 00000$	01000	00000	01000	00000
	XX0X0	$S_{0,0,1}$	$C_{0,0,1} = 00000$	00000	10000	00000	10000
	XX4X4	$S_{0,1,1}$	$C_{0,1,1} = 00000$	00000	00001	00000	00001
	XX3X3	$S_{0,2,1}$	$C_{0,2,1} = 00000$	00000	00010	00000	00010
	XX2X2	$S_{0,3,1}$	$C_{0,3,1} = 00000$	00000	00100	00000	00100
	XX1X1	$S_{0,4,1}$	$C_{0,4,1} = 00000$	00000	01000	00000	01000
1	0XX3X	$S_{1,0,0}$	$C_{1,0,0} = 10000$	00000	00000	00010	00000
	1XX4X	$S_{1,1,0}$	$C_{1,1,0} = 01000$	00000	00000	00001	00000
	2XX0X	$S_{1,2,0}$	$C_{1,2,0} = 00100$	00000	00000	10000	00000
	3XX1X	$S_{1,3,0}$	$C_{1,3,0} = 00010$	00000	00000	01000	00000
	4XX2X	$S_{1,4,0}$	$C_{1,4,0} = 00001$	00000	00000	00100	00000
	XX2X4	$S_{1,0,1}$	$C_{1,0,1} = 00000$	00000	00100	00000	00001
	XX3X0	$S_{1,1,1}$	$C_{1,1,1} = 00000$	00000	00010	00000	01000
	XX4X1	$S_{1,2,1}$	$C_{1,2,1} = 00000$	00000	00001	00000	01000
	XX0X2	$S_{1,3,1}$	$C_{1,3,1} = 00000$	00000	10000	00000	00100
	XX1X3	$S_{1,4,1}$	$C_{1,4,1} = 00000$	00000	01000	00000	00010
2	0XX1X	$S_{2,0,0}$	$C_{2,0,0} = 10000$	00000	00000	01000	00000
	2XX3X	$S_{2,1,0}$	$C_{2,1,0} = 00100$	00000	00000	00010	00000
	4XX0X	$S_{2,2,0}$	$C_{2,2,0} = 00001$	00000	00000	10000	00000
	1XX2X	$S_{2,3,0}$	$C_{2,3,0} = 01000$	00000	00000	00100	00000
	3XX4X	$S_{2,4,0}$	$C_{2,4,0} = 00010$	00000	00000	00001	00000
	X2XX3	$S_{2,0,1}$	$C_{2,0,1} = 00000$	00100	00000	00000	00010
	X4XX0	$S_{2,1,1}$	$C_{2,1,1} = 00000$	00001	00000	00000	10000
	X1XX2	$S_{2,2,1}$	$C_{2,2,1} = 00000$	01000	00000	00000	00100
	X3XX4	$S_{2,3,1}$	$C_{2,3,1} = 00000$	00010	00000	00000	00001
	X0XX1	$S_{2,4,1}$	$C_{2,4,1} = 00000$	10000	00000	00000	01000
3	0X1XX	$S_{3,0,0}$	$C_{3,0,0} = 10000$	00000	01000	00000	00000
	3X4XX	$S_{3,1,0}$	$C_{3,1,0} = 00010$	00000	00001	00000	00000
	1X2XX	$S_{3,2,0}$	$C_{3,2,0} = 01000$	00000	00100	00000	00000
	4X0XX	$S_{3,3,0}$	$C_{3,3,0} = 00001$	00000	10000	00000	00000
	2X3XX	$S_{3,4,0}$	$C_{3,4,0} = 00100$	00000	00010	00000	00000
	X3XX2	$S_{3,0,1}$	$C_{3,0,1} = 00000$	00010	00000	00000	00100
	X1XX0	$S_{3,1,1}$	$C_{3,1,1} = 00000$	01000	00000	00000	10000
	X4XX3	$S_{3,2,1}$	$C_{3,2,1} = 00000$	00001	00000	00000	00010
	X2XX1	$S_{3,3,1}$	$C_{3,3,1} = 00000$	00100	00000	00000	01000
	X0XX4	$S_{3,4,1}$	$C_{3,4,1} = 00000$	10000	00000	00000	00001
4	0X3XX	$S_{4,0,0}$	$C_{4,0,0} = 10000$	00000	00010	00000	00000
	4X2XX	$S_{4,1,0}$	$C_{4,1,0} = 00001$	00000	00100	00000	00000
	3X1XX	$S_{4,2,0}$	$C_{4,2,0} = 00010$	00000	01000	00000	00000
	2X0XX	$S_{4,3,0}$	$C_{4,3,0} = 00100$	00000	10000	00000	00000
	1X4XX	$S_{4,4,0}$	$C_{4,4,0} = 01000$	00000	00001	00000	00000
	X4X2X	$S_{4,0,1}$	$C_{4,0,1} = 00000$	00001	00000	00100	00000
	X3X1X	$S_{4,1,1}$	$C_{4,1,1} = 00000$	00010	00000	01000	00000
	X2X0X	$S_{4,2,1}$	$C_{4,2,1} = 00000$	00100	00000	10000	00000
	X1X4X	$S_{4,3,1}$	$C_{4,3,1} = 00000$	01000	00000	00001	00000
	X0X3X	$S_{4,4,1}$	$C_{4,4,1} = 00000$	10000	00000	00010	00000

Chapter 4

Performance Analysis of an Atmospheric Optical M-PPM CDMA system

4.1 Introduction

Optical wireless communication has been the subject of much research in recent years because of the increasing interest in laser satellite-ground links and urban optical wireless communication. The major source of performance degradation have been identified as the atmospheric scintillation, coherence interference due to multiscattering, dispersion etc. resulting in reduced power reception, intersignal interference as well noise due to receiver circuitry and background illumination. In this chapter we will evaluate the performance of an Atmospheric optical M-PPM CDMA system with optical orthogonal codes (OOC) and partial modified prime codes (PMP).

4.2 Signal Current at the Output of an Optical Direct Detection Receiver

The optical signal input to optical receiver is

$$S(t) = \sqrt{2P_{in}} * \exp(-j(\omega_0 t + \Delta\phi_n(t) + \theta))$$

Where P_{in} is the input optical Power, $\phi_n(t)$ is the instantaneous phase noise of transmitting laser and ω_0 is the optical carrier frequency,

The photocurrent at the output of the photodetector is-

$$i(t) = R_d S^2 \\ = R_d \bar{E} [2P_{in} * \exp(-2j(\omega_0 t + \Delta\phi_n(t) + \theta))]$$

Where R_d denotes the responsivity of the photodetector and E denotes the Expectation.

4.3 Receiver Output Statistics

The primary photocurrent within the APD produced by the incident optical field can be accurately modeled as a Poisson point process, whose rate is proportional to the instantaneous optical intensity. This photocurrent is then randomly multiplied within the

APD gain region. The probability distribution of the random APD gain has been previously derived and verified [60]. The exact formulation of the composite APD output is complex and is evaluated numerically [60]. However, the APD output has been shown to be well approximated by Gaussian statistics for an optical communication receiver [#]. Therefore, the receiver performance is completely characterized by the mean and variance of the integrated APD current conditioned on the presence or absence of the transmitted signal pulse.

4.4 Performance Analysis with Atmospheric Scintillation

In the atmospheric optical communication system using intensity modulation and direct-detection (IM/DD) the primary factor affecting the performance of the systems is intensity fluctuation that is known as the log-normal intensity scintillation. The atmospheric propagation path is characterized by molecular absorption aerosol scattering and turbulence [1, 4]. In clear weather, the molecular constituents of the atmosphere give rise to a variety of absorption bands. The atmospheric propagation loss for an L long path is $\exp(-\beta L)$, where β is the atmospheric extinction coefficient [1]. At visible wavelengths, the relation can be approximately modeled as $\exp(-VL)$, where V km is the visibility [4]. Visibility measurement can be thus used to estimate the attenuation of the optical power through the atmosphere. Line-of-sight (LOS) laser-beam propagation through the atmosphere is subject to the following undesirable effects: absorption-induced attenuation, depolarization, beam spread, angular spread, multipath spread, and time-dependent fading (Doppler spread). In clear weather at a wavelength within an atmospheric transmission window, attenuation will be minimal. In a PPM/direct- detection system, depolarization is irrelevant. Turbulence induced multipath spread is subpicosecond, and hence, negligible for the data rates of a few hundreds Mbps. We assume that the transmitter-beam divergences and the receiver field-of-view cone angle both exceed 1 mR. Thus, the beam spread and the angular spread can be neglected. Under these conditions, only attenuation (which will be modest) and scintillation need to be considered. For IM/DD systems, the received optical power can be written as

$$P(t) = X(t) P_s(t) \tag{4.1}$$

Optical Transceiver

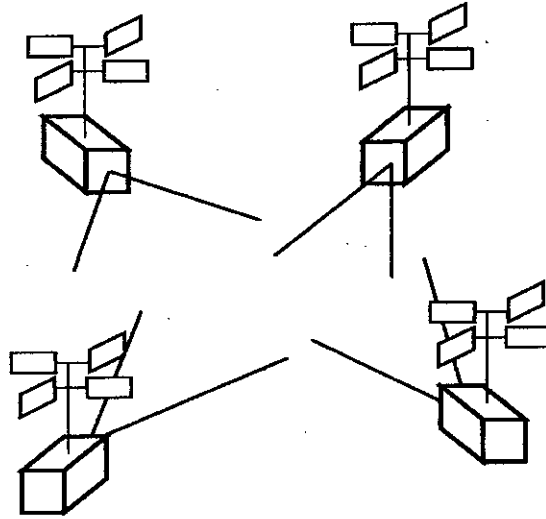


Fig.4.1 Model of atmospheric optical CDMA systems.

Where $P_s(t)$ is the received optical power without scintillation. $X(t)$ is the scintillation characterized by the stationary probability process and its probability density function can be written as [3]

$$P(X) = \frac{1}{\sqrt{2\pi\sigma_s^2 X}} \exp \left\{ -\frac{(\ln X + \frac{\sigma_s^2}{2})}{2\sigma_s^2} \right\} \quad (4.2)$$

Where the average of scintillation X is normalized to unity and σ_s^2 is logarithm variance of X . The variance of X , σ_X^2 , is equal to as $\sigma_s^2 \ll 1$ ($\sigma_X^2 = \exp(\sigma_s^2) - 1 \approx \sigma_s^2$). The variance σ_s^2 is determined by the atmospheric state.

We analyze the performance of the proposed system using APD in the chip synchronous and slot asynchronous case, where we treat the output of the APD using a Gaussian approximation. Note that optical PPM CDMA has been analyzed in fiber-optic networks in some papers, such as [58, 68].

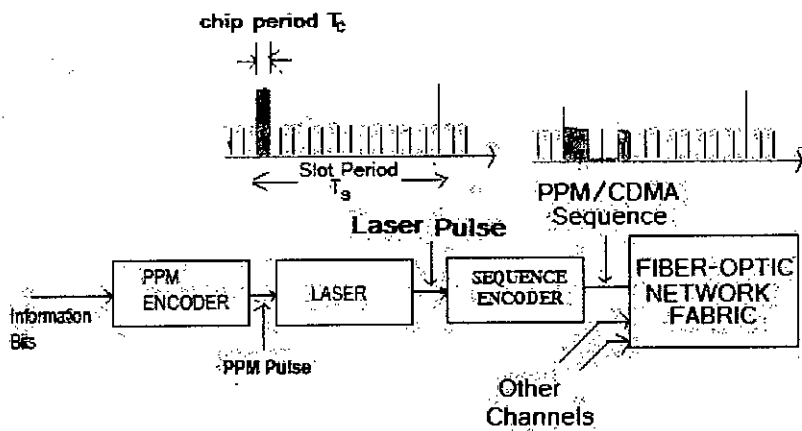


Fig.4.2 Block diagram of a PPM/CDMA transmitter and signaling format for the x th user, $L=13$, $k=3$ and $A^x = (1,1,0,0,1,0,0,0,0,0,0,0,0)$.

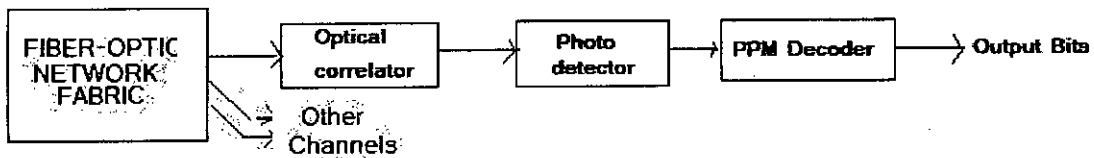


Fig.4.3 Block diagram of a PPM/CDMA receiver.

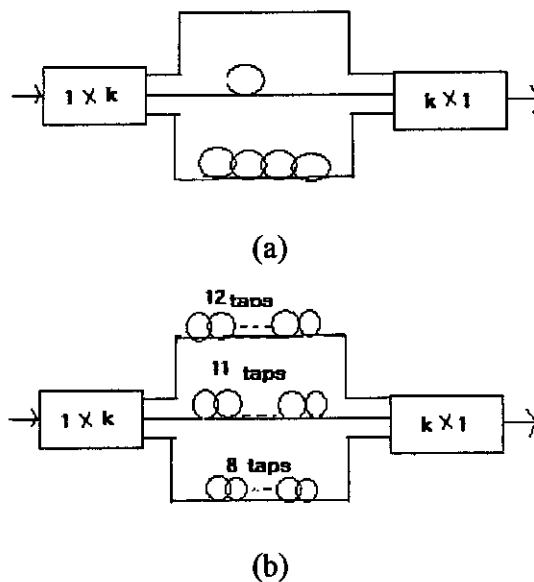


Fig.4.4 (a) Sequence Encoder and (b) Optical correlator for the x th user $L=13$, $k=3$ and $A^x = (1,1,0,0,1,0,0,0,0,0,0,0,0)$.

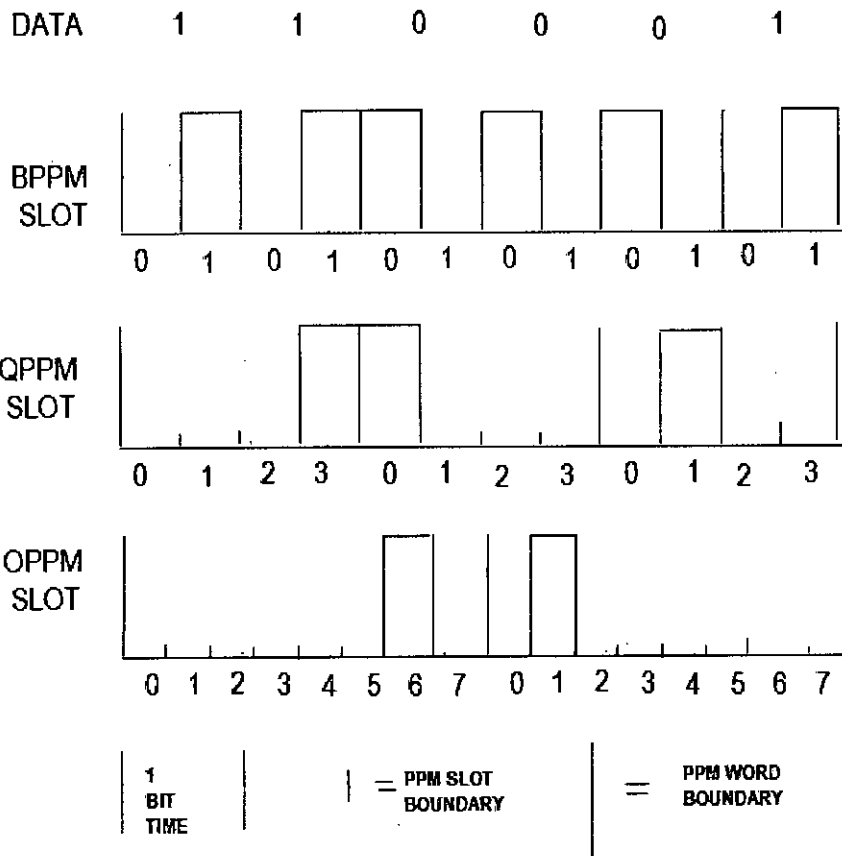


Fig.4.5. Sample bit stream in PPM modulation formats.

The probability that a specified number of photons are absorbed from an incident optical field by an APD detector over a chip interval with is given by a Poisson distribution [64-66]. The average number of absorbed photons over T_c is

$$\lambda_s = \frac{\eta P_w}{hf} \quad (4.3)$$

Where λ_s is the photon absorption rate, P_w is the received laser power, η is the APD efficiency, h is Planck's constant, and f is the optical frequency. Through an avalanche multiplication process, the APD outputs some electrons in response to the absorption of λT_c primary photons on the average: λ represents the total photon absorption rate due to signal, background, and APD bulk leakage current

$$\lambda = \begin{cases} k\lambda_s + k\lambda_b + \frac{I_b}{e} & \text{for a mark} \\ \frac{k\lambda_s}{M_e} + k\lambda_b + \frac{I_b}{e} & \text{for a space} \end{cases} \quad (4.4)$$

Where λ_s is the photon absorption rate due to the actual background light, e is an electron charge, I_b/e represents the contribution of the APD bulk leakage current to the APD output, and M_e is the modulation extinction ratio of the laser output power.

The probability that a user causes interference to the i th slot of the desired user is given by [11], [15]

$$P_i = \frac{k^2}{MF} \quad (4.5)$$

We assume the 0th user to be the desired user. We define the interference state vector at the i th slot as

$$K_i \equiv (l_i(1), l_i(2), \dots, l_i(N-1)) \quad (4.6)$$

Where

$$l_i(j) = \begin{cases} 1, & \text{if the } j\text{th user hits on the } i\text{th slot} \\ 0, & \text{otherwise} \end{cases} \quad (4.7)$$

And N is the number of users (transmitters). We also denote the output of the optical correlator in the i th slot $i \in \{0, 1, \dots, M-1\}$ by Y_i .

Assuming equally likely data, the word error probability is expressed as

$$P_e = \sum_{i=0}^{M-1} P[e|i] \Pr\{i\} \quad (4.8)$$

where $\Pr\{i\} = 1/M$ represents the occurrence probability of the i th word. Using a union bound, the conditional probability is expressed as

$$P[e|i] = \Pr\{Y_j \geq Y_i, \text{ some } j \neq i | i\} \quad (4.9)$$

$$\leq \sum_{j=0, j \neq i}^{M-1} \Pr \{Y_j \geq Y_i | i\}$$

Please note that we analyze the performance in the chip synchronous and slot asynchronous case. In this case, the conditional probability $P[e|i]$ differs for each i , because $\Pr\{Y_j \geq Y_i | i\}$ depends on the absolute value of $|i - j|$ [11]. Denoting the union bound of the word error probability P_e by P_e^U and using that $\Pr\{Y_j \geq Y_i | i\}$ depends only on the absolute value of the difference $|i - j|$, P_e^U is expressed as [11]

$$\begin{aligned} P_e^U &= \sum_{i=0}^{M-1} \sum_{j=0, j \neq i}^{M-1} \Pr\{Y_j \geq Y_i | i\} \Pr\{i\} \\ &= \frac{2}{M} \sum_{d=1}^{M-1} (M-d) \Pr\{Y_j \geq Y_i | i, |i-j|=d\} \\ &= \frac{2}{M} \sum_{d=1}^{M-1} (M-d) \Pr\{Y_d \geq Y_0 | 0\} \end{aligned} \quad (4.10)$$

Where the probability $\Pr\{Y_d \geq Y_0 | 0\}$ in (13) is evaluated as follows:

$$\begin{aligned} \Pr\{Y_d \geq Y_0 | 0\} &= \sum_{k_0 \in \mathcal{L}} \sum_{k_d \in \mathcal{L}} \Pr\{Y_d \geq Y_0 | 0, k_0, k_d\} \Pr\{k_0, k_d | 0\} \\ &= \sum_{k_0 \in \mathcal{L}} \sum_{k_d \in \mathcal{L}} \Pr\{Y_d \geq Y_0 | 0, k_0, k_d\} \Pr\{k_0, k_d | 0\} \end{aligned} \quad (4.11)$$

Where \mathcal{L} is the set of all the interference vectors.

The upper bound on the conditional probability in (14) is given by

$$\Pr\{Y_d \geq Y_0 | 0, k_0, k_d\} \leq \Pr\{Y_d \geq Y_0 | 0, k_0 = 0, k_d\} \quad (4.12)$$

Substituting (15) into (14), we get the following conditional equation [11]:

$$\begin{aligned} \Pr\{Y_d \geq Y_0 | 0\} &\leq \sum_{k_0 \in \mathcal{L}} \sum_{k_d \in \mathcal{L}} \Pr\{Y_d \geq Y_0 | 0, k_0 = 0, k_d\} \Pr\{k_0, k_d\} \\ &= \sum_{k_d \in \mathcal{L}} \Pr\{Y_d \geq Y_0 | 0, k_0 = 0, k_d\} \Pr\{k_d\} \end{aligned} \quad (4.13)$$

Please note that $\Pr\{k_d\}$ is expressed as

$$\Pr\{k_d\} = \left(\frac{K^2}{MF}\right)^{|k_d|} \left(1 - \frac{K^2}{MF}\right)^{N-1-|k_d|} \quad (4.14)$$

Substituting (16) and (17) into (13), we get the upper bound on P_e^U as follows:

$$P_e^U \leq (M-1) \sum_{k_d \in \mathcal{L}} \left(\frac{K^2}{MF}\right)^{|k_d|} \left(1 - \frac{K^2}{MF}\right)^{N-1-|k_d|} \cdot \Pr\{Y_d \geq Y_0 | 0, k_0 = 0, k_d\} \quad (4.15)$$

Where $|k_d|$ is the number of nonzero elements in k_d . At an optical CDMA receiver, the optical intensity received at the mark positions of the code sequence for the desired channel is summed up at the last chip by the optical correlator consisting of a set of optical delay lines inversely matched to the pulse spacings [67]. The output of the optical correlator is converted into the electrical signal by the APD. The receiver integrates the APD output over the last chip interval T_c . Using a Gaussian approximation of the APD output, the probability $\Pr\{Y_d \geq Y_0 | 0, k_0 = 0, k_d\}$ in (18) is derived as

$$\begin{aligned} \Pr\{Y_d \geq Y_0 | 0, k_0 = 0, k_d\} &= \int_0^\infty p(X_0) \int_0^\infty p(X_1) \dots \int_0^\infty p(X_{N-1}) \cdot \\ &\int_{-\infty}^\infty \frac{1}{\sqrt{2\Pi\sigma_d^2(X)}} e^{-\frac{(x-\mu_d(x))^2}{2\sigma_d^2(X)}} \int_{-\infty}^\infty \frac{1}{\sqrt{2\Pi\sigma_0^2(X)}} e^{-\frac{(y-\mu_0(x))^2}{2\sigma_0^2(X)}} dy dx dX_0 dX_1 \dots dX_{N-1} \end{aligned} \quad (4.16)$$

Where $X = \{X_0, X_1, \dots, X_{N-1}\}$ and X_i is the scintillation for the i th user. The means and the variances of Y_d and Y_0 , μ_d , μ_0 and σ_d^2 , σ_0^2 are derived, respectively, as

$$\mu_d(X) = GT_c \left[\sum_{i=1}^{N-1} l_d(i) X_i \lambda_{s,i} + \frac{KX_0 \lambda_{s,0}}{M_e} + \sum_{i=1}^{N-1} (K - l_d(i)) \frac{X_i \lambda_{s,i}}{M_e} + K\lambda_b + \frac{I_b}{e} \right] + \frac{T_c J_s}{e} \quad (4.17)$$

$$\mu_0(X) = GT_c \left[KX_0 \lambda_{s,0} + \sum_{i=1}^{N-1} \frac{KX_i \lambda_{s,i}}{M_e} + K\lambda_b + \frac{I_b}{e} \right] + \frac{T_c J_s}{e} \quad (4.18)$$

$$\sigma_{th}^2(X) = G^2 F_e T_c \left[\sum_{i=1}^{N-1} l_d(i) X_i \lambda_{s,i} + \frac{K X_0 \lambda_{s,0}}{M_e} + \sum_{i=1}^{N-1} (K - l_d(i)) \frac{X_i \lambda_{s,i}}{M_e} + K \lambda_b + \frac{I_b}{e} \right] + \frac{T_c I_s}{e} + \sigma_{th}^2 \quad (4.19)$$

$$\sigma_{th}^2(X) = G^2 F_e T_c \left[K X_0 \lambda_{s,0} + \sum_{i=1}^{N-1} \frac{K X_i \lambda_{s,i}}{M_e} + K \lambda_b + \frac{I_b}{e} \right] + \frac{T_c I_s}{e} + \sigma_{th}^2 \quad (4.20)$$

Here, $\lambda_{s,i}$ is the photon-absorption rate of the i th user, G is the average APD gain, I_s is the APD surface leakage current, and F_e is the excess noise factor given by

$$F_e = k_{eff} G + \left(2 - \frac{1}{G} \right) (1 - k_{eff}) \quad (4.21)$$

Where k_{eff} is the APD effective ionization ratio, and σ_{th}^2 is the variance of thermal noise written as

$$\sigma_{th}^2 = \frac{2k_B T_c T_r}{(e^2 R_L)} \quad (4.22)$$

Where k_B is Boltzmann's constant, T_r is the receiver-noise temperature, and R_L is the receiver-load resistor. Therefore, the BER of the atmospheric optical M-ary PPM CDMA systems is derived as

$$P_b \leq \frac{M}{2(M-1)} P_c^U \quad (4.23)$$

Please note that our performance involves two levels of bounds and a Gaussian approximation and that (4.16) is the average over log normal power of Gauss exceeding another.

Chapter 5

Result and Discussion

5.1 Introduction

The simulation results are presented and discussed in this chapter. The bit error rate (BER) performance, sensitivities and penalties are calculated as functions of the relevant receiver and atmospheric parameter for direct detection M-PPM OCDMA system with optical orthogonal codes and partial modified prime codes. Also the performance comparisons of system with two different codes have been presented in details.

5.2 Results and Discussion

In order to determine the effect of atmospheric scintillation and system with different code on the performance of direct detection M-ary PPM schemes, it has been evaluated numerically the bit error rate (BER) performance as a function of average signal count per bit considering the effect of shot noise, thermal noise, spontaneous emission noise and laser phase noise. The nominal values of the parameters which are used through the calculation are given in Table 5.1

First the bit error rate performance have been calculated for different value of average signal count per bit with APD gain, wavelength and optical bandwidth as a parameter and plotted against received laser power. Then the effect of atmospheric scintillation is considered and the BER performance is evaluated for M-ary PPM OCDMA system with OOC's and PMP code. The effect of atmospheric scintillation on the Bit error rate (BER) performance is determined in the forms of power penalty and the results due to multi user's access are compared for different types of codes.

Table 5.1: Nominal Parameters of Optical Wireless Communication Link

Parameter Name	Value
Background Noise, P_b	-45dBm
Wavelength, λ	830nm
APD Gain, G	100
Receiver Noise Temperature, T_r	1100 ⁰ k
Surface Leakage current, I_s	10 nA
Bulk Leakage Current, I_b	0.1 nA
Bit Rate, B_r	1 Gbps
Modulation Extinction Ratio, M_e	100
Receiver Load Resistor, R_L	1030
APD Quantum efficiency, \square	0.6
APD effective Ionization Ratio, k_{eff}	0.02

We show some numerical results using the following parameters: OOC is with $F=19$ and $K=3$, the wavelength of the optical carrier is $0.83 \mu\text{m}$, the background noise is $P_b=-45\text{dBm}$ and the bit rate is $R_b=1\text{Gbps}$. We set the variance of scintillation to 0.01, 0.1, 0.3, and 0.5 that corresponds to the turbulence strength parameter C_n^2 of 3.08×10^{-15} , 3.08×10^{-14} , 9.23×10^{-14} and 1.54×10^{-13} for plane waves, and 7.57×10^{-15} , 7.57×10^{-14} , 2.27×10^{-13} , and 3.79×10^{-13} for spherical waves, respectively, where the path length is 250m. Note that P_w denotes the unit received laser power in a delay-line of optical correlator without scintillation. We use typical APD parameters in Table I. We assume the photon absorption rate and the logarithm variance of the scintillation to be same for all the users, respectively

Fig. 5.1, 5.2, 5.3, 5.4 and 5.5 shows the BER versus the received laser power without scintillation P_w for M-ary PPM CDMA system where σ_s^2 is the logarithm variance of the scintillation. We can see that the OCDMA system can realize communications when σ_s^2 is smaller than or equal to 0.1. This is because the proposed system employs PPM instead of OOK, and thus, there is no need to adapt the receiver threshold. When σ_s^2 is larger than 0.1 we need to use forward error correction codes (FECs). We can also see that the error floor exists when the σ_s^2 is larger than or equal to 0.1. This reason is as follows. When σ_s^2 is large and there exists the effects of scintillation, there is possibility that the interference power even in the regime of high power. Note that we assume the photon absorption rate to be same for all users. Thus, the error floor exists in Fig. 1. Note also that, when there exists no effects of scintillation, the error floor exists for systems with the number of interference users larger than or equal to the code weight.

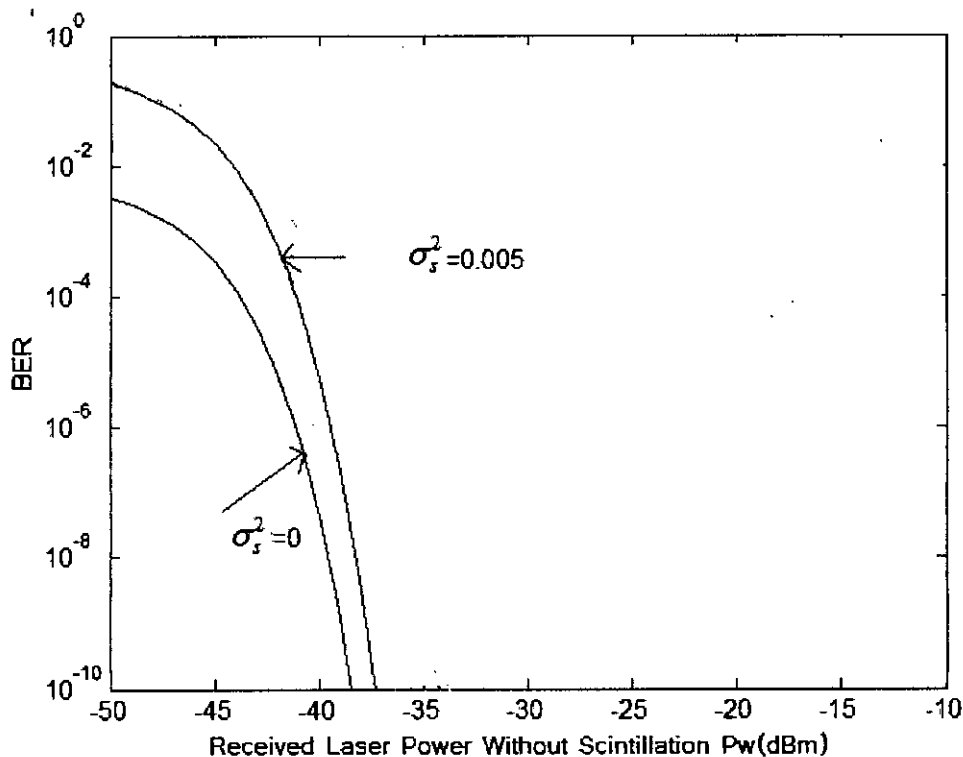


Fig.5.1 BER Versus the received laser power without scintillation P_w for four-ary PPM-CDMA ($M=4, \sigma_s^2=0, \sigma_s^2=0.005$)

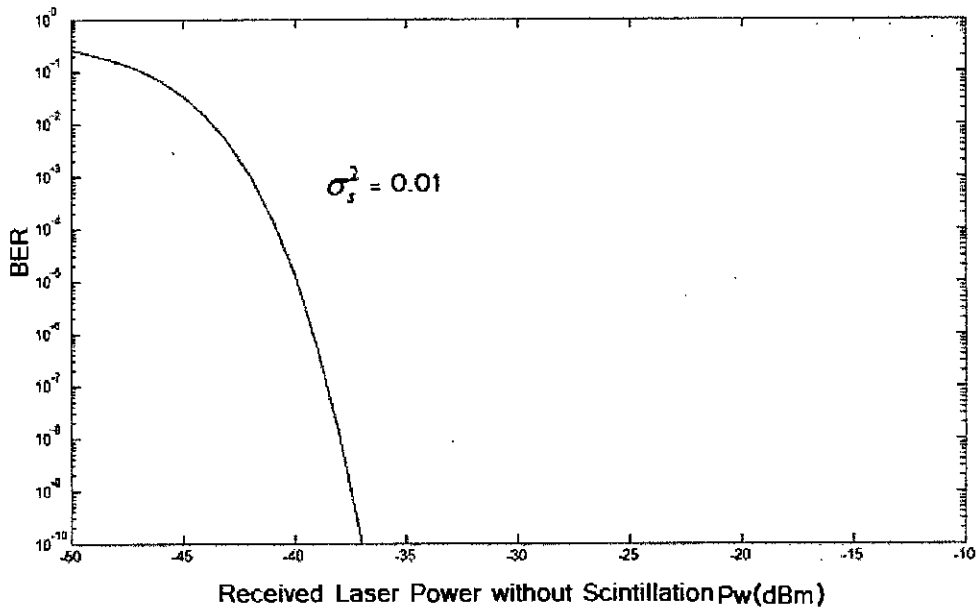


Fig.5.2 BER Versus the received laser power without scintillation Pw for four-ary PPM CDMA ($M=4$, $\sigma_s^2=0.01$)

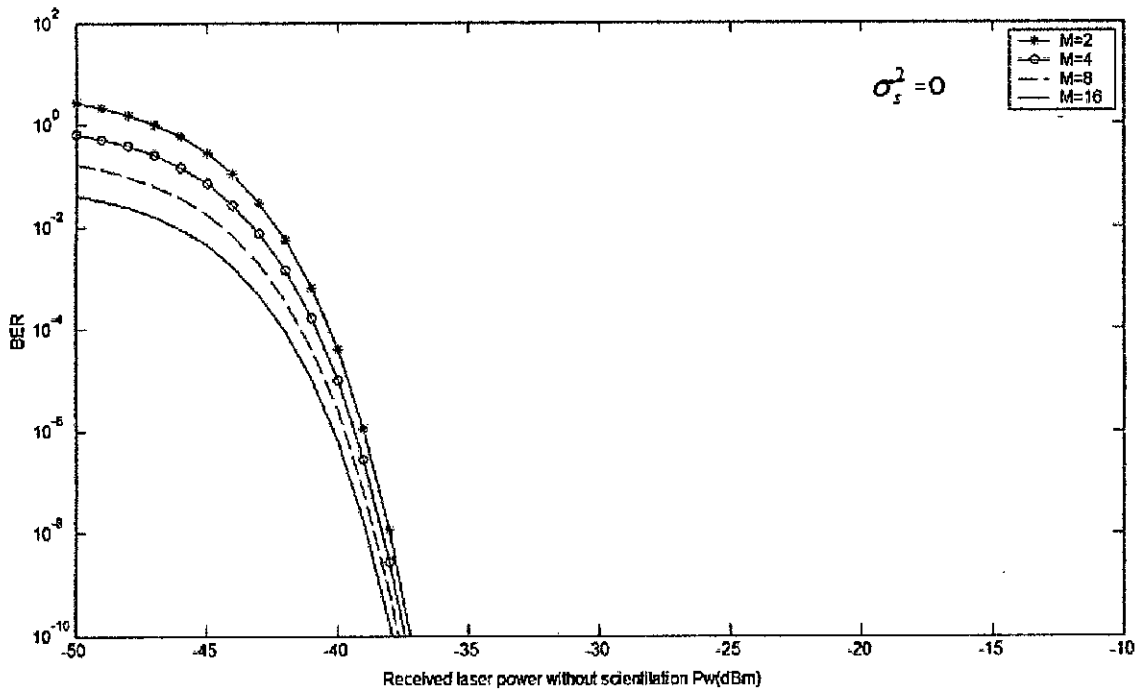


Fig.5.3 BER Versus the received laser power without scintillation P_w for M-ary PPM CDMA ($\sigma_s^2=0$)

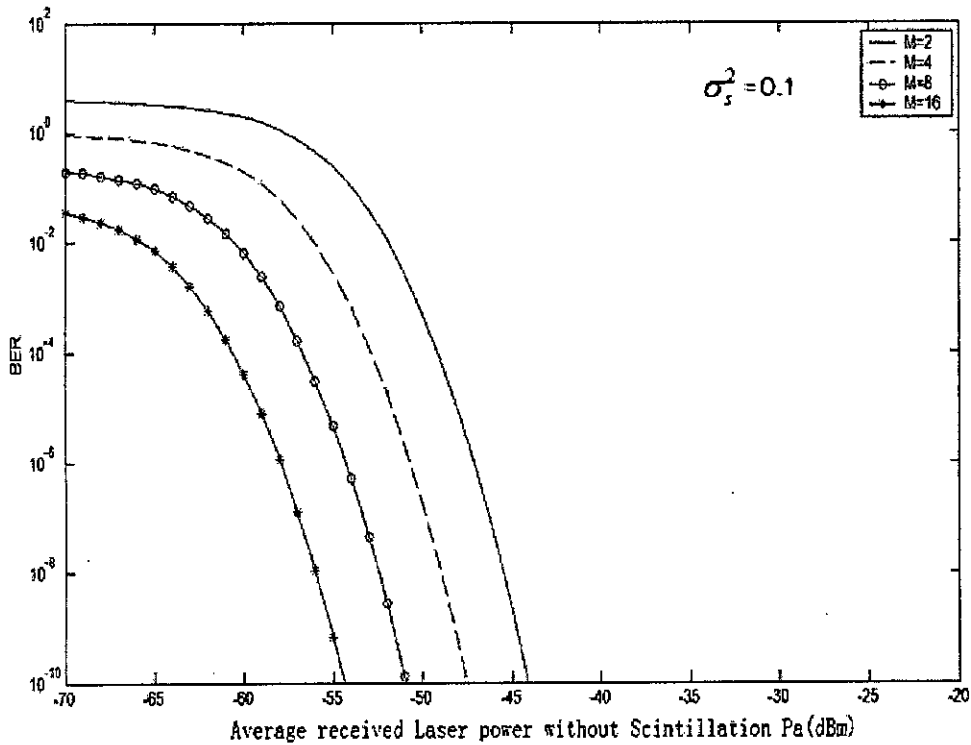


Fig.5.4 BER Versus the average received laser power without scintillation P_w for M -ary PPM CDMA ($\sigma_s^2=0.1$)

Fig.5.4 shows the BER versus the average received laser power without scintillation P_a for M -ary PPM-CDMA systems, where σ_s^2 is 0.1. The average received laser power

$$\text{without scintillation } P_a \text{ is given by } P_a = \frac{K}{MF} P_w. \quad (5.1)$$

We can see that the performance of the proposed system is improved with the increase of M . This is because when M becomes larger, P_w becomes larger for the same value of M as shown in (5.1). Note again that as M increases at the same bit rate, the chip rate becomes higher.

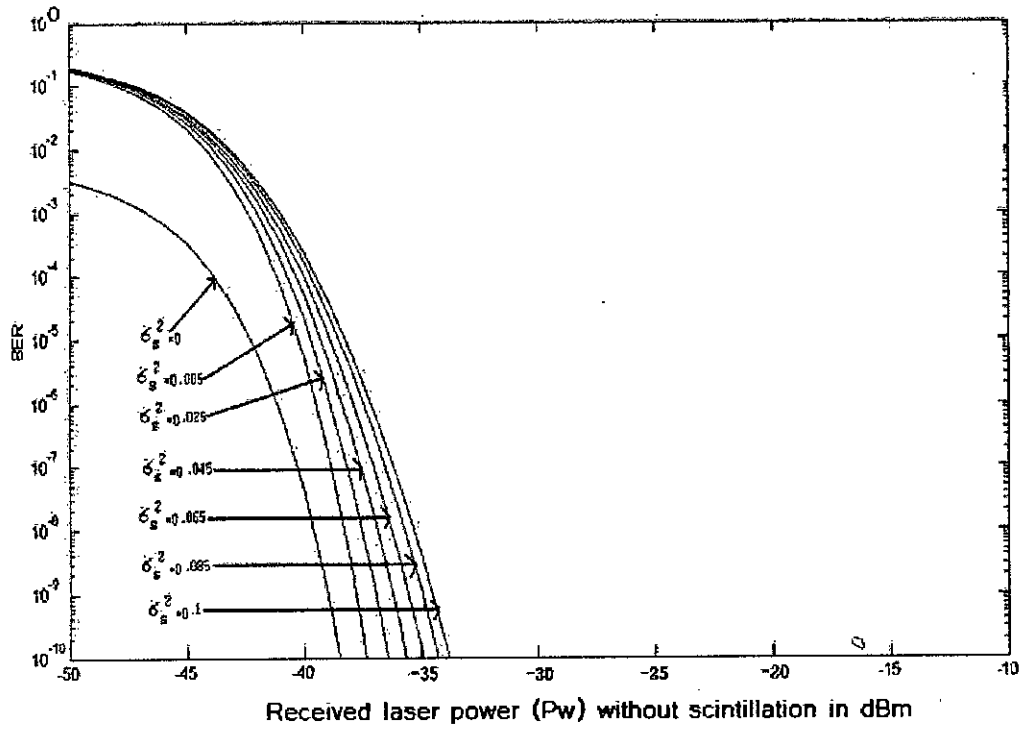


Fig.5.5 BER Versus the received laser power without scintillation P_w for four-ary PPM CDMA in the presence of different values of σ_s^2

Fig.5.5 shows the BER versus the received laser power without scintillation P_w for 4-ary PPM-CDMA systems, considering the different values of scintillation σ_s^2 .

We can see that the performance of the proposed system is better for smaller σ_s^2 , when σ_s^2 is large there is a possibility that the interference power is larger than the desired user's even in the regime of high power.

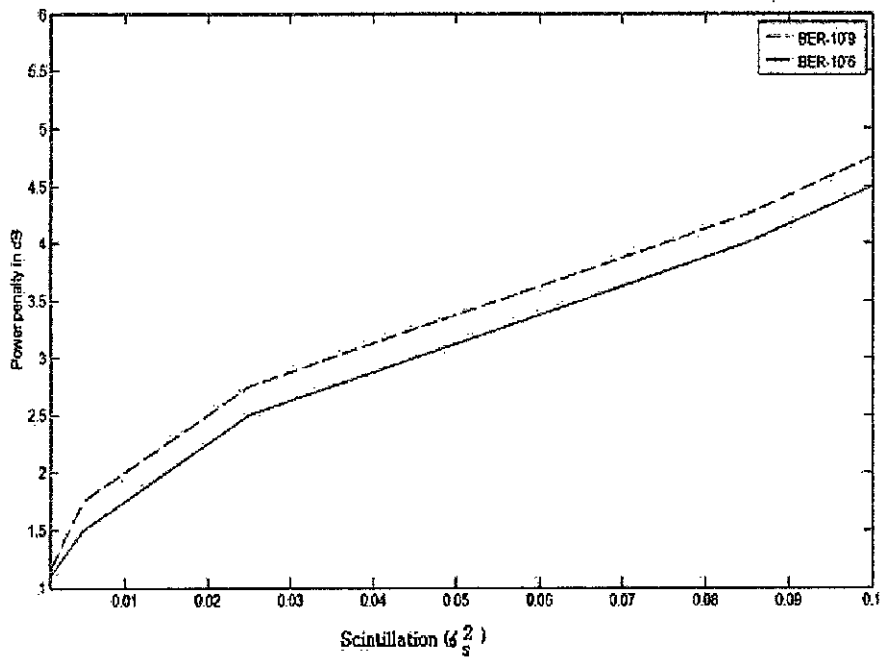


Fig.5.6 Power penalty as a function of variance of scintillation (M=4)

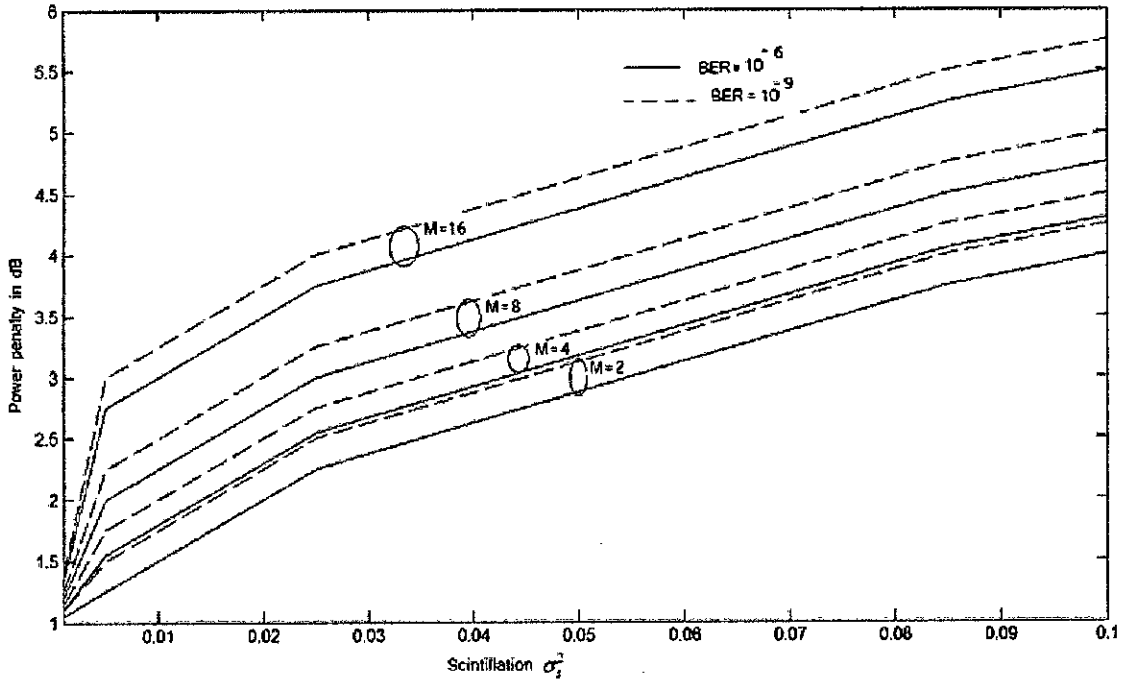


Fig.5.7 Power penalty as a function of variance of scintillation for M-ary PPM

Figs. 5.6 and 5.7 shows the penalty suffered by the system due to atmospheric scintillation at BER 10^{-9} and 10^{-6} as a function of scintillation variance, σ_s^2 . It is found that the penalty is significantly higher at higher values of σ_s^2 .

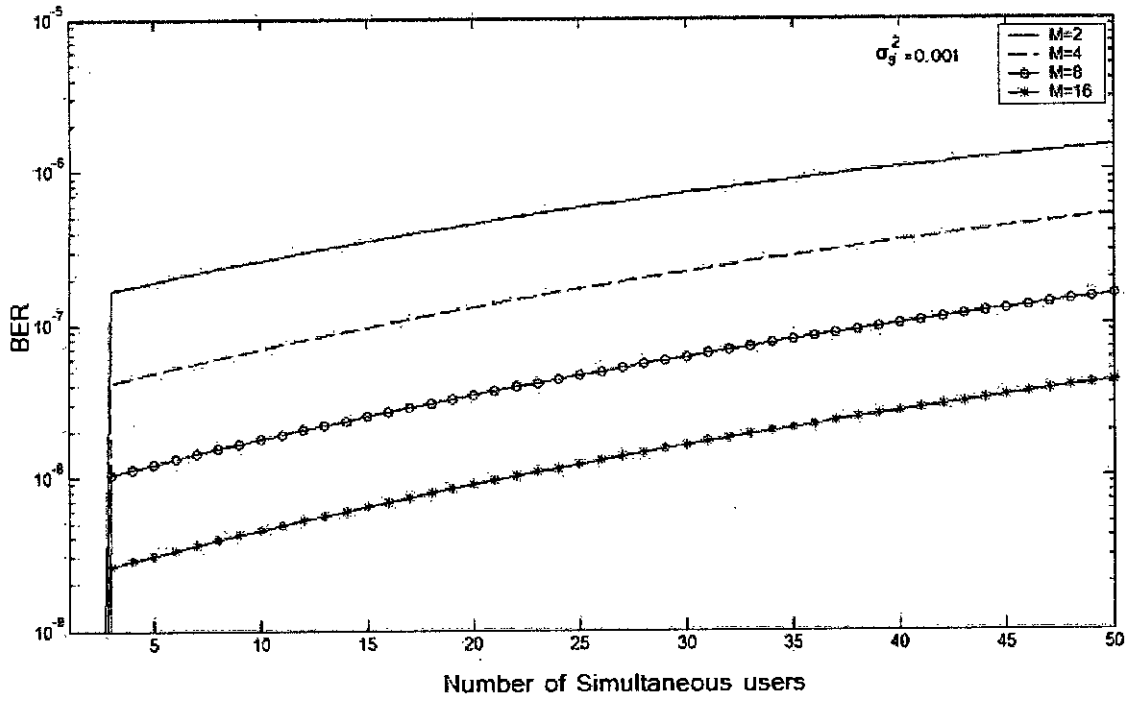


Fig. 5.8 BER Versus Number of Users for M-ary PPM-CDMA ($\sigma_s^2 = 0.001$)

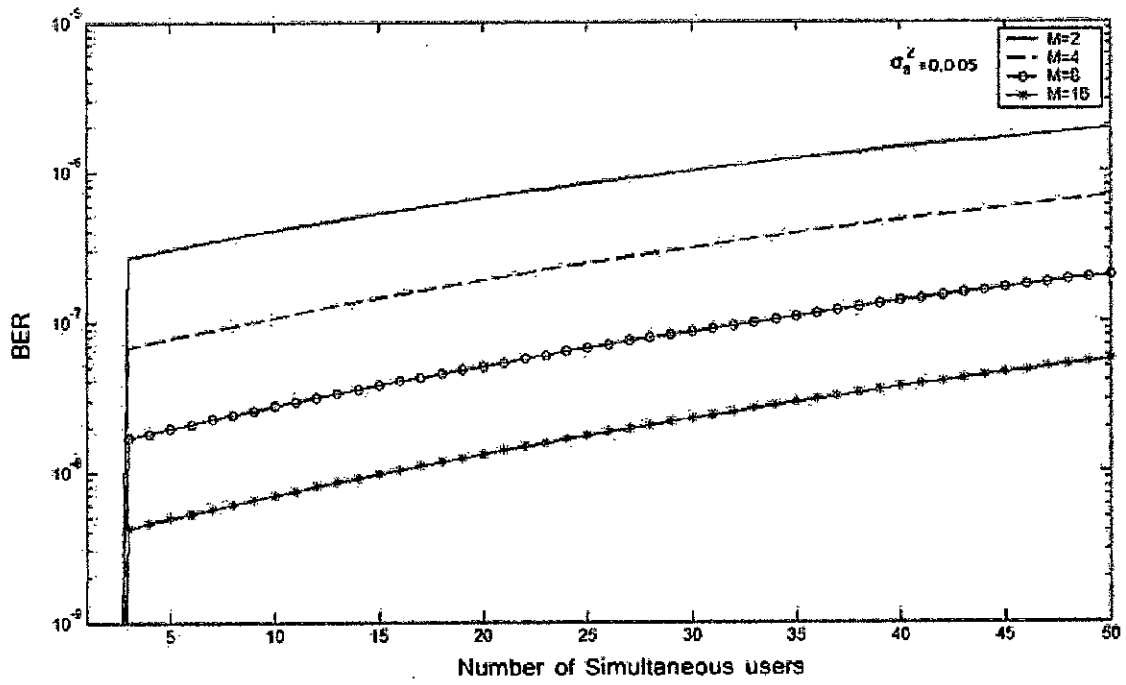


Fig. 5.9 BER Versus Number of Users for M-ary PPM-CDMA ($\sigma_s^2 = 0.005$)

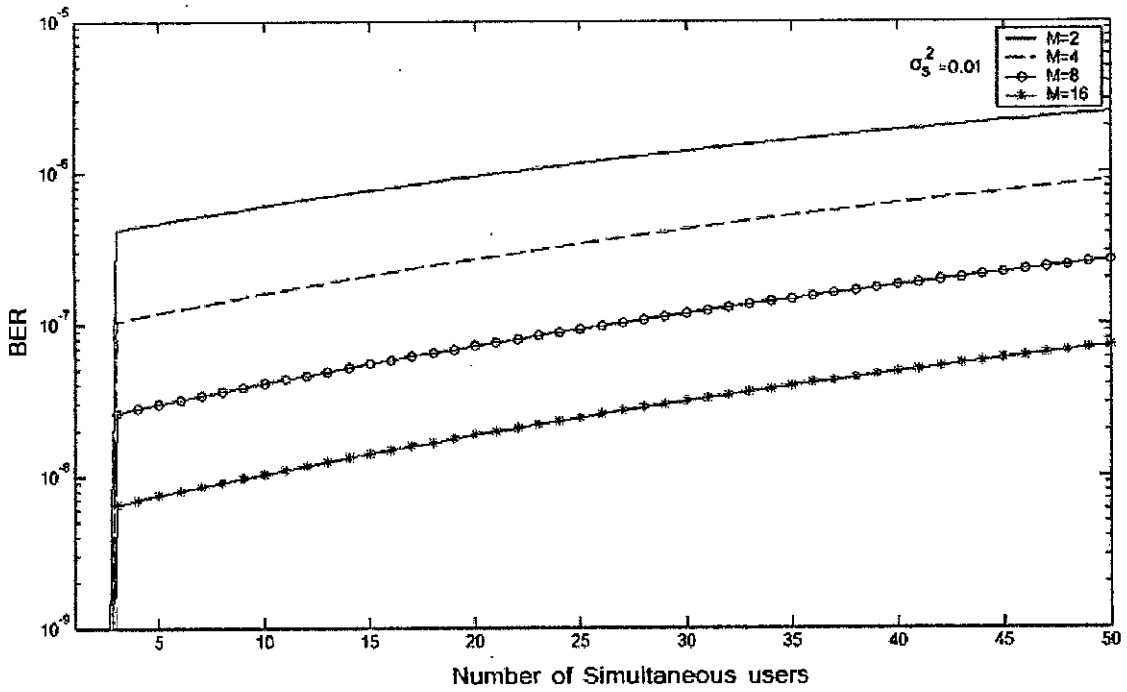


Fig.5.10 BER Versus Number of Users for M-ary PPM-CDMA ($\sigma_s^2 = 0.01$)

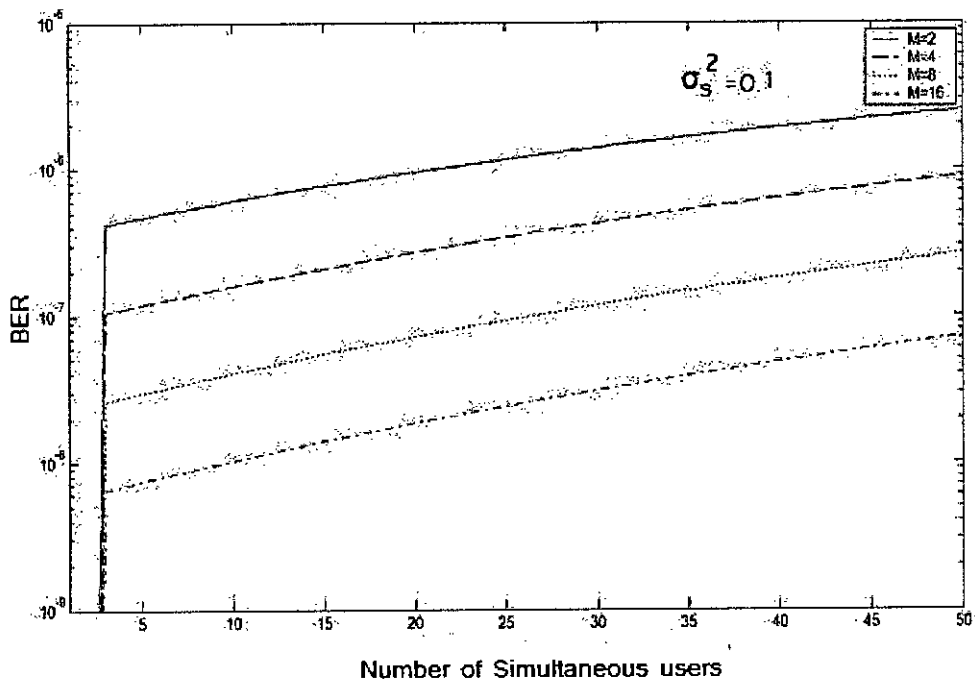


Fig.5.11 BER Versus Number of Users for M-ary PPM-CDMA ($\sigma_s^2 = 0.1$)

Figs. 5.8, 5.9, 5.10 and 5.11 shows the BER versus the number of simultaneous users for M-ary PPM-CDMA systems, considering the different values of scintillation. It is found that system performance degrade with the increase of number of active users. We can see that the performance of the proposed system is better for larger M.

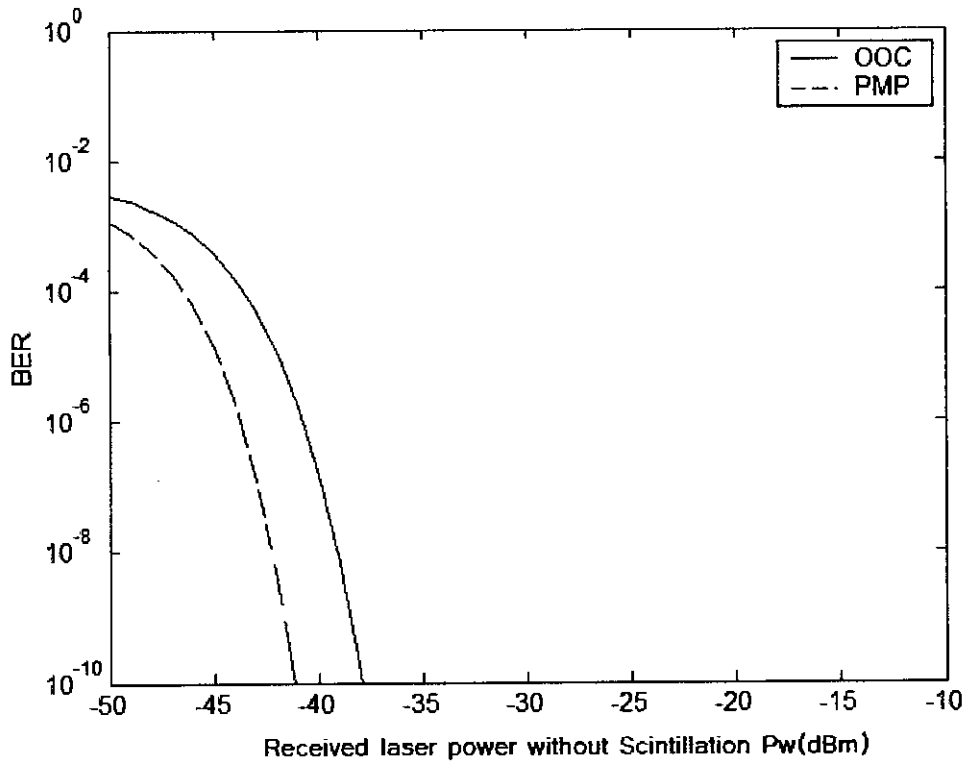


Fig.5.12 BER Versus the received laser power without scintillation P_w considering M-PPM CDMA system with OOC's and PMP codes ($M=4$, $N=3$, $\sigma_s^2=0.1$)

56/9/21

Fig.5.12 shows the BER versus the received laser power without scintillation P_w for 4-ary PPM CDMA system with optical orthogonal codes and partial modified prime codes, where σ_s^2 is the logarithm variance of the scintillation. We can see that for the same atmospheric scintillation system with partial modified prime codes shows better performance than system with optical orthogonal codes.

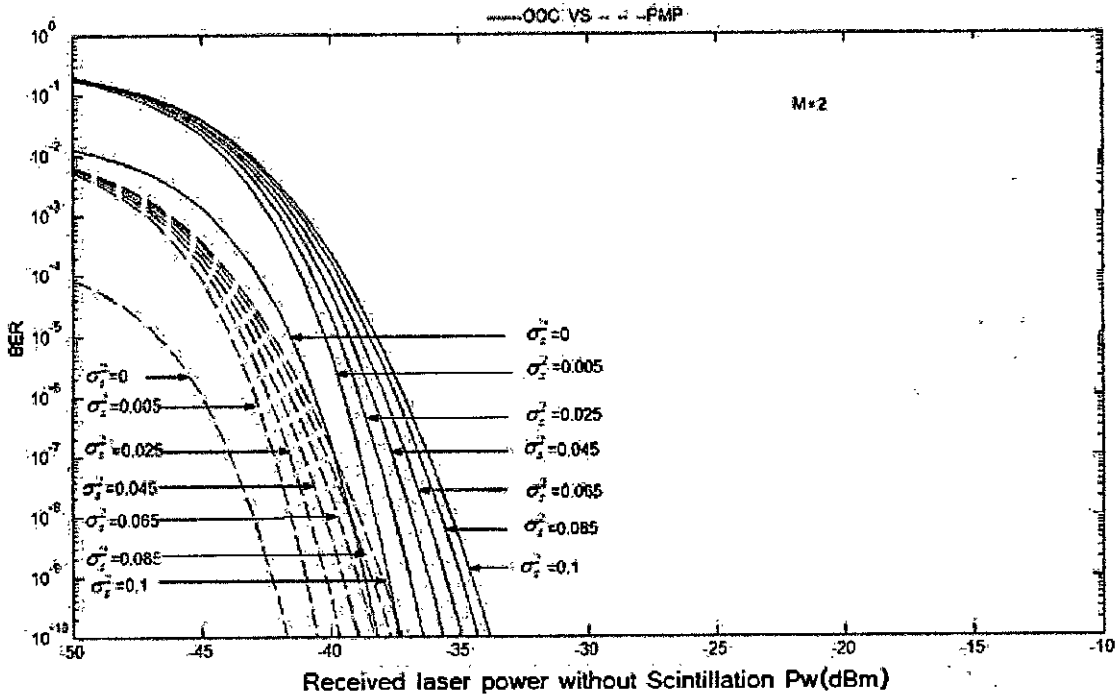


Fig.5.13 BER Versus the received laser power without scintillation Pw considering M-PPM CDMA system with OOC's and PMP codes in the presence of different values of σ_y^2 (M=2, N=3)

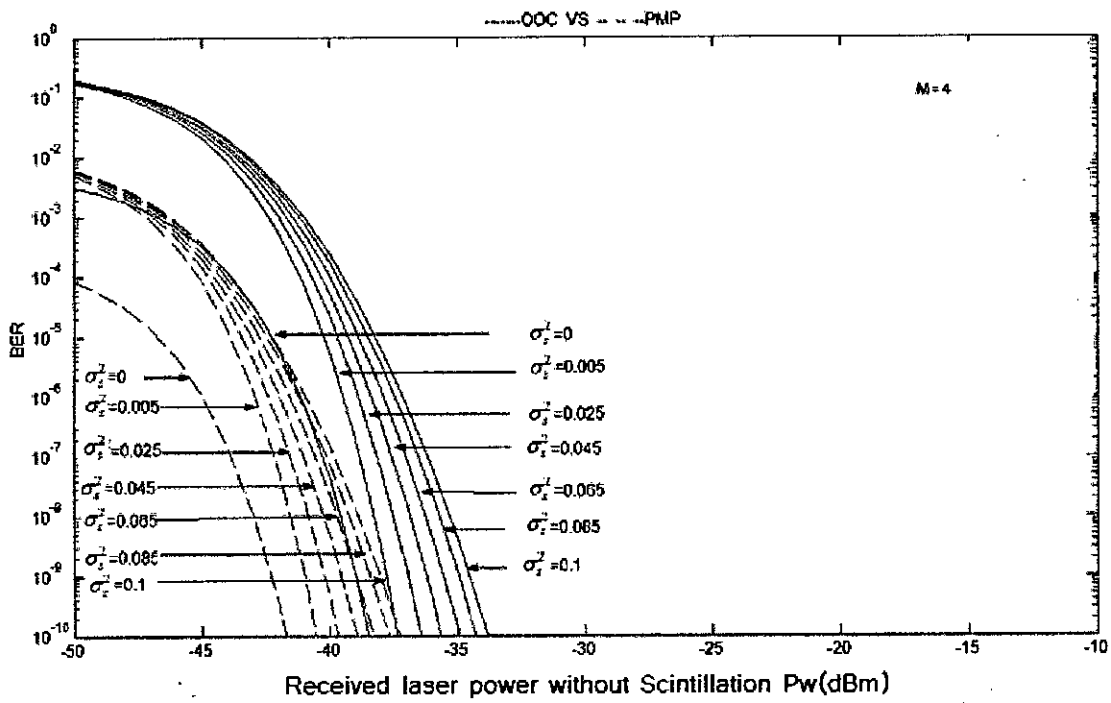


Fig.5.14 BER Versus the received laser power without scintillation Pw considering M-PPM CDMA system with OOC's and PMP codes in the presence of different values of σ_s^2 (M=4, N=3)

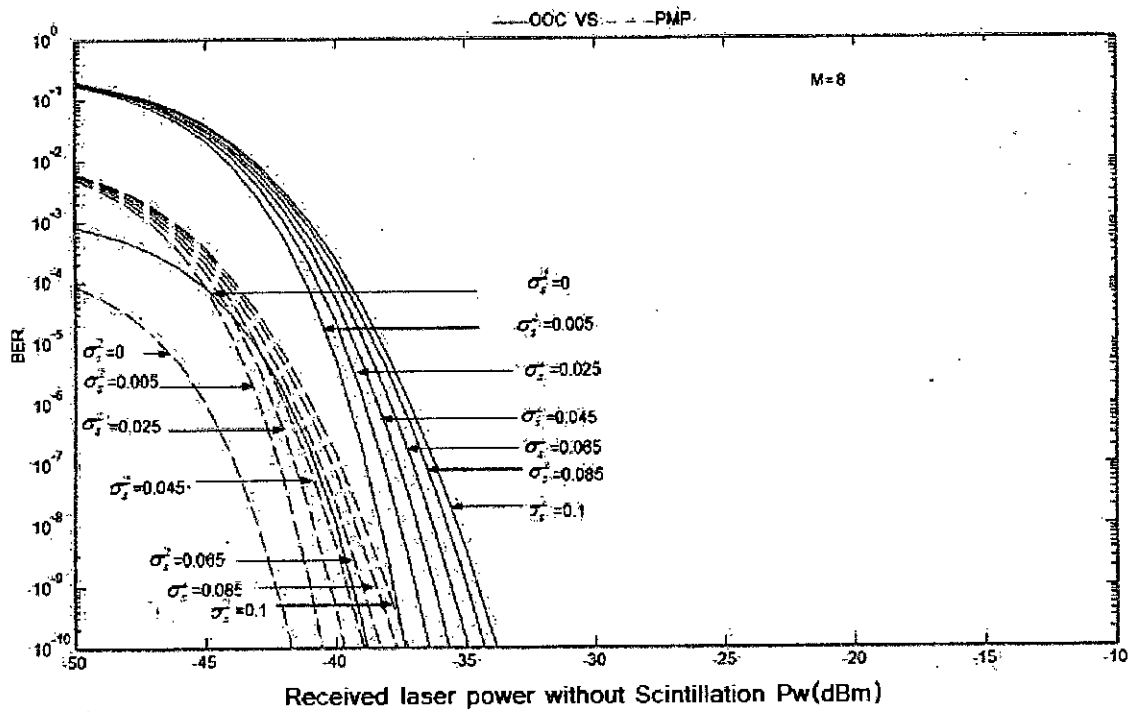


Fig 5.15 BER Versus the received laser power without scintillation Pw considering M-PPM CDMA system with OOC's and PMP codes in the presence of different values of σ_s^2 (M=8, N=3)

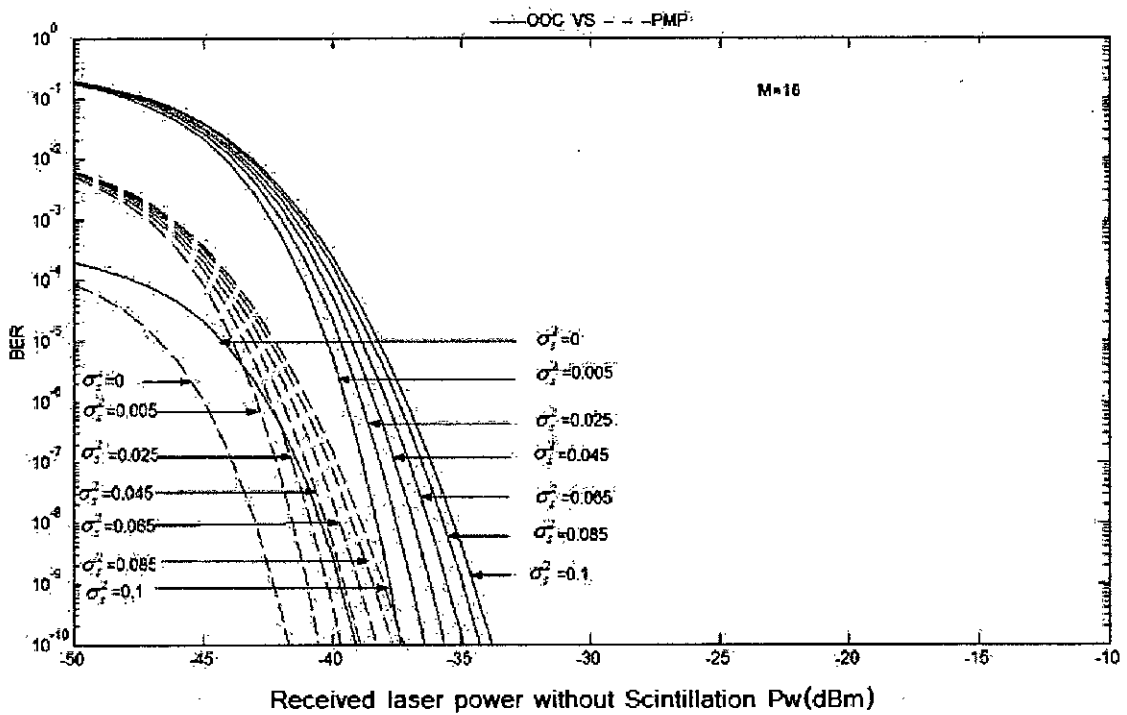


Fig.5.16 BER Versus the received laser power without scintillation P_w considering M-PPM CDMA system with OOC's and PMP codes in the presence of different values of σ_s^2 ($M=16, N=3$)

Figs.5.13, 5.14, 5.15 and 5.16 shows the BER versus the received laser power without scintillation P_w for M-ary PPM-CDMA systems with optical orthogonal codes and partial modified prime codes, considering the different values of scintillation σ_s^2 .

We can see that the performance of the proposed system is better for smaller σ_s^2 and higher M, when σ_s^2 is large there is a possibility that the interference power is larger than the desired user's even in the regime of high power. We can also see that system performance with partial modified codes is better than the system with optical orthogonal codes.

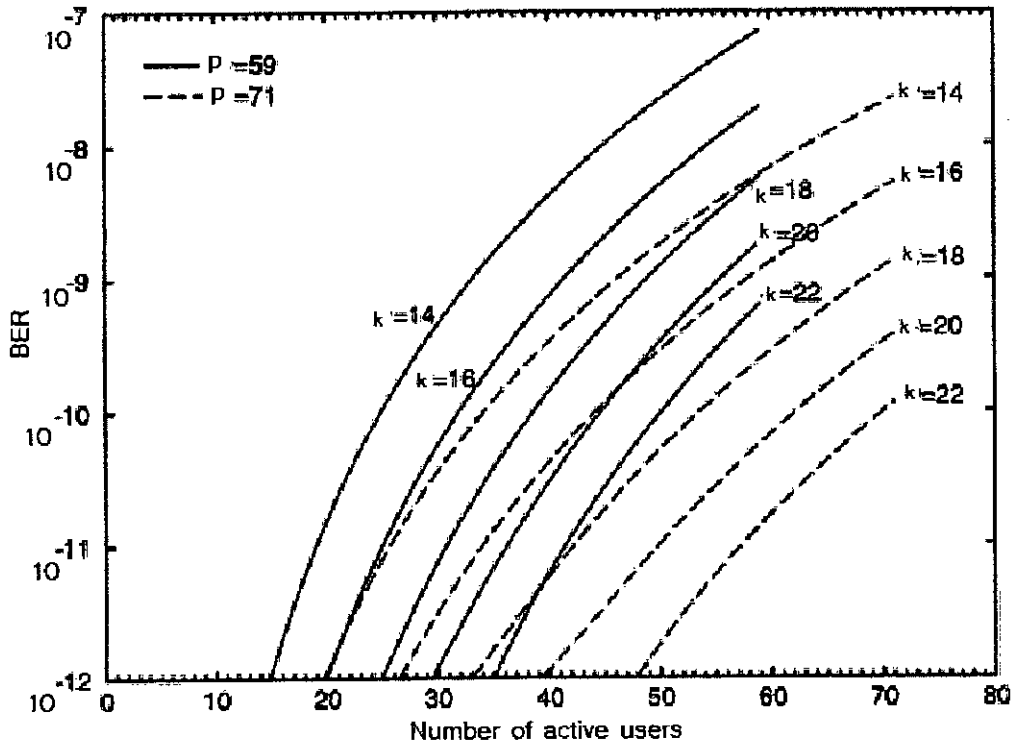


Fig.5.17 BER versus the number of active users for OCDMA systems with PMP codes

Fig.5.17 shows the BER versus the number of active users as a function of p and k , where $F = p^2$. We can find that, for $BER \leq 1 \times 10^{-9}$, using the proposed code can significantly reduce the k compared with employing a prime code of $k = p$. For example, to support 71 active users with $BER < 10^{-9}$, only $k = 20$ is required for the PMP code rather than $k = 71$ for a prime code, so the system cost or complexity can be reduced. Moreover, the BER is decreased with the increase of F for a given k , e.g., a PMP code with $k = 14$ and $p = 71$ can achieve the same BER as the PMP code of $k = 18$ and $p = 59$ for 59 active users, at the expense of a bandwidth increased by 44.8%.

Chapter 6

Conclusion

6.1 Summary

A detailed analytical approach is presented to evaluate the bit error rate performance degradation of a wireless optical link in the presence of atmospheric scintillation with M-ary PPM schemes. The effect of atmospheric scintillation on the BER performance determined in the forms of power penalty and the results compared for different types of codes and optimum system parameters determined.

- Simulation results are satisfactorily agreed with the expected results.
- It is found that the performance of optical direct detection M-PPM systems is very sensitive to atmospheric scintillation.
- There is a significant degradation in BER performance due to atmospheric scintillation and the penalty is higher for higher value of scintillation variation
- It is also observed that higher order PPM offers better performance.
- The numerical results confirm the superior performance of the PMP-coded OCDMA system in comparison to OOC-OCDMA system even under the scintillation effect.
- The result is useful in determining the receive power level of the system to guarantee a given receiver symbol error performance.

6.2 Future Scope of Work

1. Future research can be carried out on the effect of atmospheric scintillation on a WDM free-space optical link.
2. Research can be initiated to investigate the impact of atmospheric dispersion on a single channel and multi-channel optical free space communication system.
3. The proposed code-design procedure can be extended to construct special PMP codes, such as variable-length PMP codes and nonconstant-weight PMP codes.
4. Forward error correction coding can be applied to minimize the effect of atmospheric scintillation and to improve the performance of a atmospheric optical communication system.

Reference:

- [1] Binder B.T, Yu P.T., Shapiro J.H., and Bounds J.K., "An atmosphere optical ring network,"IEEE Trans. Commun, vol. 38, PP. 74-81, Jan 1990.
- [2] A. M. Street et al., "Indoor optical wireless systems - a review," Opt. and Quantum Elect., no. 29, pp. 349-78,1997.
- [3] J. M. Khan and J. R. Barry, "Wireless infrared communications," Proc. IEEE, vol. 85, pp. 265-298, Feb. 1997.
- [4] H. A. Willebrand and B. S. Ghuman, "Fiber optics without fiber," IEEE Spectrum, vol. 38, pp. 40-45, Aug. 2001.
- [5] P. R. Prucnal, M. A. Santoro, and S. K. Sehgal, "Ultrafast all-optical synchronous multiple access fiber networks," IEEE J. Select. Areas Commun., vol. SAC-4, pp. 1484–1493, Dec. 1986.
- [6] Naoya Wada and Ken-Ichi Kitayama, "A 10 Gb/s Optical Code Division Multiplexing Using 8-Chip Optical Bipolar Code and Coherent Detection." J. Lightwave Technol, vol. 17, no. 10, pp. 1758-1765 October 1999.
- [7] P. R. Prucnal, M. A. Santoro, and T. R. Fan, "Spread spectrum fiber-optic local area network using optical processing," J. Lightwave Technol., vol. LT-4, pp. 547–554, May 1986.
- [8] Williams and I. Millar, "The IrDA Platform," Proc. 2nd Int'l. Wksp. Mobile Multimedia Commun., Bristol Univ., England, 1995.
- [9] Subir Kumar Sarkar, "Optical fibers and fiber optic communication systems," 2nd ed., S. Chand & company ltd, Ramnagar, New Delhi, 2003.
- [10] S. E. Miller and I. Kaminow, "Optical fiber telecommunication" 11. New York Academic Press, pp. 808, 1988.
- [11] John M. Senior, "Optical Fiber Communications," 2nd ed. Prentice Hall, New Delhi-2003.

- [12] G. P. Agrawal, "Nonlinear Fiber Optics," 3rd ed., Academic press, San Diego, CA, 2001.
- [13] R. P. Khare, "Fiber optics and and optoelectronics," 1st ed., Oxford Uni. press, 2004.
- [14] W. Huang, J. Takaynagi, T. Sakanaka and M. Nakagawa, "Atmospheric optical communication system using subcarrier PSK modulation." Proc. IEEE ICC, pp.1597-1601, 1993.
- [15] Ohtsuki Tomoaki, Khan M. Joseph, "BER performance of turbo-coded PPM CDMA systems on optical fiber," IEEE J. Light Wave Technology, vol. 18, No. 12, Dec. 2000.
- [16] Shalaby H. M. H , "Performance analysis of optical synchronous CDMA commun. systems with PPM signaling", IEEE Trans. on Commun., vol. 43, PP. 624-634, Feb1995.
- [17] Sato K., Ohtsuki T., Uehara H., and Sasase I., "Effect of imperfect slot synchronization on direct-detection optical synchronous CDMA communication system with PPM signaling , " IEEE J. Light wave technology, vol. 14, PP. 1963-1969, Sep 1996.
- [18] Abshire J. B, "Performance of OOK and low-order PPM modulations in optical communication when using APD-based receivers, " IEEE Trans. Commun, vol.32, pp. 1140-1143, Oct. 1984.
- [19] Arbab Vahid R., Saghari Poorya, Haghi Mahta, Ebrahimi Paniz, and Alan E. Willner, "Increasing the bit rate in OCDMA systems using PPM techniques," Optics Express vol. 15, No. 19, September 2007.
- [20] Ohtsuki Tomoaki, "Performance analysis of atmospheric optical PPM CDMA systems." IEEE J. Light Wave Technology, Vol. 21, PP. 406-411, Feb 2003.
- [21] Jim Song, Chongcheng Fan, "A Simplified Dispersion Limit Formula for IM/DD Systems and its Comparison with Experimental Results" J. Lightw. Techno., vol. 13, no. 3, pp. 546-550, March 1995.
- [22] Tomoaki Ohtsuki, "Performance Analysis of Direct-Detection Optical Asynchronous CDMA Systems with Double Optical Hard-Limiters," J. Lightw. Techno., vol. 15, No. 3, pp. 452-457, March 1997.

- [23] S. Benedetto and G. Olmo, "Performance Evaluation of Coherent Optical Code Division Multiple Access," *Electron. Lett.*, vol. 27, pp. 2000-2002, Oct. 1991.
- [24] D. Zaccarin, M. Kavehrad, "Performance Evaluation of Optical CDMA Systems Using Non-Coherent Detection and Bipolar Codes" *J. Lightw. Techno.*, vol. 12, no. 1, pp. 96-105, Jan 1994.
- [25] M. Kavehrad and D. Zaccarin, "Optical code-division-multiplexed systems based on spectral encoding of noncoherent sources," *J. Lightw. Techno.*, vol. 13, no. 3, pp. 534-545, Mar. 1995.
- [26] Sato K., Ohtsuki T., Uehara H., and Sasase I., "Performance of optical direct-detection CDMA systems using prime sequence codes," in *Proc. ICC'95*, Seattle, WA, PP.1312-16.
- [27] Lam A.W. and Hussin A. M., "Performance of DD OCDMA communication systems with avalanche photodiodes," *IEEE Trans. on commun.*, vol. 40, PP. 810-820, April 1992.
- [28] Lin Cheing-Hong, Wu Jingshown, Taso Hen-Wai and Yang Chun-Liang, "Spectral amplitude-coding optical CDMA system using mach-zender interferometers", *IEEE J.Light Wave Technology*, vol. 23, No. 4, April 2005.
- [29] Salehi and C.A Brackett, "Code division multiple-access technique in optical fiber networks-part II: System performance analysis," *IEEE Trans. on Commun.*, vol. 37, pp. 834-842, Aug. 1989.
- [30] K. Kitayama, H. Sotobayashi and N. Wada, "Optical code division multiplexing (OCDMA) and its application to photonic networks," *IEICE Trans. Fundamentas*, vol. E82-A, pp. 2616-2626, Dec. 1999.
- [31] M. Dale and R.M. Gagliardi, "Analysis of fiber optic code-division multiple access," Tech. Rep. CSI Tech. Rep. 92-06-10, Univ. Southern Calif. Los Angels CA. 1992.
- [32] D. Brady and S. Verdu, "A Semi Classical Analysis of Optical Code Division Multiple Access," *IEEE Trans. Commun.*, vol. 39, pp. 85-94, Jan. 1991.
- [33] D. E. Carlson, "Bit-Oriented Data Link Control Procedures," *IEEE Trans. Commun.*, vol. Com-28, no. 4, pp. 455-67, 1980.

- [34] P. R. Prucnal, M. A. Santoro, and T. R. Fan, "Spread spectrum fiber-optic local area network using optical processing," *J. Lightw. Technol.*, vol. LT-4, pp. 547-554, May 1986.
- [35] H. M. Kwon, "Optical orthogonal code-division multiple access system-part I: APD noise and thermal noise," *IEEE Trans. Commun.*, vol. 42, pp. 2470-2479, July 1994.
- [36] F. R. K. Chung, J. A. Salehi, and V. K. Wei, "Optical orthogonal codes: Design, analysis and applications," *IEEE Trans. Inform. Theory*, vol. 35, pp. 595-604, May 1989.
- [37] W. C. Kwong, P. A. Perrier, and P. R. Prucnal, "Performance comparison of asynchronous and synchronous code-division multiple-access techniques for fiber-optic local area networks," *IEEE Trans. Commun.*, vol.39, pp. 1625-1634, Nov. 1991.
- [38] C. S. Weng and J. Wu, "Perfect difference codes for synchronous fiber optic CDMA communication systems," *J. Lightw. Technol.*, vol. 19, pp. 186-194, Feb. 2001.
- [39] X. Zhou, H. H. M. Shalaby, C. Lu, and T. Cheng, "Code for spectral amplitude coding optical CDMA systems," *Electronics Letters*, vol. 36, no. 8, pp. 728-729, Apr.13th, 2000
- [40]J.-G. ZHANG, "Flexible optical fiber CDMA networks using strict optical orthogonal codes for multimedia broadcasting and distribution applications," *IEEE Trans. Broadcasting*, vol. 45, pp. 106-115, 1999.
- [41] J.-G. ZHANG, "Design of a special family of optical CDMA address codes for fully asynchronous data communications," *IEEE Trans. Commun.*, vol. 47, pp. 967-973, 1999.
- [42] J.-G. ZHANG, "Address codes for use in all-optical CDMA systems," *Electron. lett.*, vol. 32, pp. 1154-1156, 1996."
- [43] G. Yang, "Variable-weight optical orthogonal codes for CDMA networks with multiple performance requirements," *IEEE Trans. Commun.*, vol. 44, no. 1, pp. 47-55, Jan. 1996.
- [44] L. Nguyen, T. Dennis, B. Aazhang and J. F. Young, "Experimental demonstration of bipolar codes for optical spectral amplitude CDMA communication," *J. Lightwave Technol.*, vol. 15, pp. 1647-1653, Sept.1997.
- [45] G. Yang and T. Fuja, "Optical orthogonal codes with unequal auto- and cross correlation constraints," *IEEE Trans. Inform. Theory*, vol. 41, no.1, pp. 96-106, Jan. 1995.

- [46] D. V. Sarwate and M. B. Pursley, "Crosscorrelation properties of pseudorandom and related sequences," *Proc. IEEE*, vol. 68, pp. 593–619, 1980.
- [47] T. Dennis and J. F. Young, "Optical implementation of bipolar codes," *IEEE J. Quantum Electron.*, vol. 35, pp. 287–291, Mar. 1999.
- [48] L. Nguyen, B. Aazhang, and J. F. Young, "All-optical CDMA with bipolar codes," *Electron. Lett.*, vol. 31, pp. 469–470, Mar. 1995.
- [49] Cho-Chin Yang, Jen-Fa Huang and Shin-Pin Tseng, "Optical CDMA Network Codecs Structured with Sequence Codes over Waveguide-Grating Routers" *IEEE Photonics Technology Letters*, vol. 16, No.2, pp.641-643, February-2004.
- [50] C.-L. Lin and J. Wu, "Channel interference reduction using random Manchester codes for both synchronous and asynchronous fiber-optic CDMA systems," *J. Lightwave Technol.*, vol. 18, pp. 26–33, Jan. 2000.
- [51] F. Liu, M. M. Karbassian, H. Ghafouri-Shiraz, "Novel family of prime codes for synchronous optical CDMA." *Opt Quant Electron*, vol. 39, pp. 79–90, 2007.
- [52] Wing C. Kwong, Guu-Chang Yang, and Jian-Guo Zhang, " 2^n Prime-sequence codes and coding architecture for optical code division multiple access." *IEEE Transactions on Commun.*, vol. 44, no. 9, pp. 1152-1162 September 1996.
- [53] A. Holmes and R. Syms, "All-optical CDMA using "quasiprime" code," *J. Lightwave Technol.*, vol. 10, no. 2, pp. 279-286, Feb. 1992.
- [54] Jian-Guo Zhang and Wing C. Kwong, "Design of Optical Code-Division Multiple-Access Networks with Modified Prime Codes," *Ulm, Germany, June 29 -July 4, ISIT 1997,*
- [55] J.-G. ZHANG and G. PICCHI, "Tunable prime-code encoder/decoder for all-optical CDMA applications," *Electron. Lett.*, vol. 29, pp. 1211-1212, 1993.
- [56] T. Ohtsuki, K. Sato, I. Sasase, and S. Mori, "Direct-detection optical synchronous CDMA systems with double optical hard-limiters using modified prime sequence codes," in *Conf. Rec. GLOBECOM'95, Singapore*, pp. 2156–2160, Nov. 1995.
- [57] K. P. Jackson, S. A. Newton, B. Moslehi, M. Tur, C. C. Culter, J. W. Goodman, and H. J. Show, "Optical fiber delay-line signal processing," *IEEE Trans. Microwave Theory Tech.*, vol. MTT-33, pp. 193–210, Mar. 1985

- [58] E. D. J. Smith, R. J. Blaikie, and D. P. Taylor, "Performance enhancement of spectral amplitude-coding optical CDMA using pulse-position modulation," *IEEE Trans. Commun.*, vol. 46, no. 3, pp. 1176–1185, Sep. 1998.
- [59] Kiran and D. Tse. "Effective interference and effective bandwidth of linear multiuser receivers in asynchronous CDMA systems." *IEEE Trans. Info. Theory*, vol. 46(4) pp. 1426–1447, July 2000.
- [60] L. B. Nelson and H. V. Poor, "Performance of multiuser detection for optical CDMA-Part I: Error probabilities," *IEEE Trans. Commun.*, vol. 43, no. 11, pp. 2803–2811, Nov. 1995.
- [61] H. M.H. Shalaby, "A comparison between the performance of number state and coherent-state optical CDMA in lossy photon channels," *IEEE J. Select Areas Commun.*, vol. 13, pp. 592–602, Apr 1995.
- [62] K. Iversen and D. Hampicke, "Comparison and classification of all optical CDMA systems for future telecommunication networks," in *All-Optical Communication Systems: Architecture, Control, and Network Issues*, V. W. Chan, R. A. Cryan, and J. M. Senior, Eds., *Proc. SPIE*, vol. 2614, pp. 110–121, 1995.
- [63] Hossam M. H. Shalaby, "Synchronous Fiber-Optic CDMA Systems with Interference Estimators" *J. Lightwave Technol.*, vol. 17, No. 11, pp. 2268–2275 November 1999.
- [64] L. B. Nelson and H. V. Poor, "Performance of multiuser detection for optical CDMA—Part II: Asymptotic analysis," *IEEE Trans. Commun.*, vol. 43, pp. 3015–3024, Dec. 1995.
- [65] E. Marom and O. G. Ramer, "Encoding-decoding optical fiber network," *Electron. Lett.*, vol. 14, no. 3, pp. 48–49, 1978.
- [66] L. B. Nelson and H. V. Poor, "Performance of multiuser detection for optical CDMA—Part II: Asymptotic analysis," *IEEE Trans. Commun.*, vol. 43, pp. 3015–3024, Dec. 1995.
- [67] H. M. H. Shalaby and E. A. Sourour, "Co-channel interference cancellation in optical synchronous CDMA communication systems," in *Proc. IEEE 3rd Int. Symp. Spread Spectrum Tech. Applications (ISSSTA '94)*, Oulu, Finland, pp. 579–583, July 4–6, 1994.

- [68] Shalaby and H.M.H, "A performance analysis of optical overlapping PPM-CDMA communication systems." *IEEE/OSA J. Lightwave Technol*, vol.17, pp. 426–433, 1999.
- [69] Suzuki Hiroshi, "Trial of optical beam network," *Optronics JST*, vol. 215, pp. 155-159, 1999.
- [70] Tong, D.T.K., Wu M.C., "Optical Beam forming network with true-time delay using mode-locked super modes and dispersive fiber," vol. 7, no.11, pp. 40-41, Aug. 1995.
- [71] Zou Wei, H. M. H. Shalaby, and H. Ghafouri-Shiraz, "Modified Quadratic Congruence Codes for Fiber Bragg-Grating-Based Spectral-Amplitude-Coding Optical CDMA Systems," *Journal of lightwave Tech.*, vol. 19, no. 9, September 2001.
- [72] Kazuo Hagimoto and Kazuo Aida, "Multigigabit-per-second optical baseband transmission system," *Journal of lightwave Tech.*, vol. 6, no.11, November 1988.
- [73] S. Fujita, N. Henmi, I. Takano, M. Yamaguchi, T. Torikai, T. Su-Zaki, S. Takano, H. Ishigara and M. Shikada, "10 Gbit/s-80km optical fiber transmission experiment using a directly modulated DFG LD and high speed InGaAs-APD," presented at OFC'88, 1988
- [74] Complete wireless solution for all application, AirlinX communication, Inc.
- [75] Ibrahim G., Sensening J., Al-Mahadawi T., "Dynamic reflection of RF signals from fluorescent lights: Their spectral analysis and effects on backscattered RFID tag signals," *Sarnoff Symposium IEEE*, vol. April 30 2007-May 2 2007, pp.1-5.
- [76] R. Narasimhan, M. D. Audeh, J.M. Khan, "Effect of electronic-ballast fluorescent lighting on wireless infrared links," *IEEE proc. Optoelectronics*, vol. 143, no.6, pp.348-354 December 1996.
- [76] Gffller F. R and Bapst U. H, "Wireless in-house data communication via diffuse infrared radiation", *proc. IEEE*, vol. 67, pp. 1474-1486, 1979.
- [77] Khan J.M, Krause W. J and Carruthers J. B, "Experimental characterization of non-directed indoor infrared channels", *IEEE Trans. Commun.*, vol. 43 (4), pp. 1613-1623, 1995.
- [78] Kortzin M.D, "Short range communication using diffusely scattered radiation", PhD dissertation, North western university, June 1981.

APPENDIX A

SIMPLIFICATION OF PROBABILITY OF BIT ERROR RATE (BER) FOR M-ARY PULSE POSITION MODULATION (MPPM)

For the Pulse Position Modulation (PPM) technique, probability of bit error rate can be written as $\text{Prob}_{\text{M-PPM}}(\text{bit error}) = N_{\text{BS}} (1 - \text{Prob}(\text{CSC}))$ (A1)

Where, CSC denotes "correct slot choice" and

$$N_{\text{BS}} = \frac{k2^{k-1}}{2^k - 1} \quad (\text{A2})$$

N_{BS} is the average number of bit error per receiver error and k is the number of bits sent per word.

The probability of correct slot choice can be written as,

$$\text{Prob}(\text{CSC}) = \int_{-\infty}^{\infty} P_{X_s}(x) \left[\int_{-\infty}^{\infty} P_{X_{ns}}(y) dy \right]^{N-1} dx \quad (\text{A3})$$

Here the receiver probability densities P_{X_s} and $P_{X_{ns}}$ are normal with means $\langle X_s \rangle$ and $\langle X_{ns} \rangle$ and variances are $\sigma_{X_s}^2$ and $\sigma_{X_{ns}}^2$ respectively.

We know that probability in normal distribution is given by,

$$p(x) = \frac{1}{\sqrt{2\pi\sigma^2_x}} e^{-\frac{(x-\bar{x})^2}{2\sigma^2_x}} \quad (\text{A4})$$

\bar{x} = Mean value

Equation (B3) can be written in the following form

$$\begin{aligned} \text{Prob}(\text{CSC}) &= \int_{-\infty}^{\infty} p(X_s) \left[\int_{-\infty}^{\infty} p(X_{ns}) dX_{ns} \right]^{M-1} dX_s \\ &= \int_{-\infty}^{\infty} p(X_s) \left[\int_{-\infty}^{X_s} \frac{1}{\sqrt{2\pi\sigma_{ns}^2}} e^{-\frac{(X_{ns}-\bar{X}_{ns})^2}{2\sigma_{ns}^2}} dX_{ns} \right]^{M-1} dX_s \end{aligned} \quad (\text{A5})$$

Let $\frac{X_{ns} - \bar{X}_{ns}}{\sqrt{2\sigma_{ns}^2}} = y$ then $dX_{ns} = \sqrt{2\sigma_{ns}^2} dy$

As $X_{ns} = -\infty$ then $y = -\infty$

$X_{ns} = X_s$ then $y = \frac{X_s - \bar{X}_{ns}}{\sqrt{2\sigma_{ns}^2}}$

Equation (B5) becomes,

$$\begin{aligned}
\text{Prob(CSC)} &= \int_{-\infty}^{\infty} p(X_s) \left[\int_{-\infty}^{\frac{(X_s - \overline{X_{ns}})}{\sqrt{2\sigma_{ns}}}} \frac{1}{\sqrt{\pi}} e^{-y^2} dy \right]^{M-1} dX_s \\
&= \int_{-\infty}^{\infty} \frac{1}{\sqrt{2\pi\sigma_s}} e^{-\frac{(X_s - \overline{X_s})^2}{2\sigma_s^2}} \left[\int_{-\infty}^{\frac{(X_s - \overline{X_{ns}})}{\sqrt{2\sigma_{ns}}}} \frac{1}{\sqrt{\pi}} e^{-y^2} dy \right]^{M-1} dX_s
\end{aligned} \tag{A6}$$

With the following substitution,

$$\begin{aligned}
\text{Let } \frac{X_s - \overline{X_{ns}}}{\sqrt{2\sigma_{ns}}} &= z \\
\Rightarrow X_s &= \sqrt{2\sigma_s} z + \overline{X_s} \\
\Rightarrow dX_s &= \sqrt{2\sigma_s} dz
\end{aligned}$$

$$\begin{aligned}
\text{As } X_s = -\infty &\Rightarrow z = -\infty \\
X_s = \infty &\Rightarrow z = \infty
\end{aligned}$$

$$\begin{aligned}
\frac{X_s - \overline{X_{ns}}}{\sqrt{2\sigma_{ns}}} &= \frac{\sqrt{2}z\sigma_s + \overline{X_s} - \overline{X_{ns}}}{\sqrt{2\sigma_{ns}}} \\
&= \frac{X_s - \overline{X_{ns}}}{\sqrt{2\sigma_{ns}}} + \frac{\sigma_s}{\sigma_{ns}} z
\end{aligned}$$

$$= \delta + uz$$

$$= x'$$

Where

$$\delta = \frac{X_s - \overline{X_{ns}}}{\sqrt{2\sigma_{ns}}}, \quad u = \frac{\sigma_s}{\sigma_{ns}} \quad \text{and} \quad x' = \delta + uz$$

From equation (B6)

$$\text{Prob (CSC)} = \int_{-\infty}^{\infty} \frac{1}{\sqrt{\pi}} e^{-z^2} \left[\int_{-\infty}^{x'} \frac{1}{\sqrt{\pi}} e^{-y^2} dy \right]^{M-1} dX_s \tag{A7}$$

Now,

$$\int_{-\infty}^{x'} \frac{1}{\sqrt{\pi}} e^{-y^2} dy = \int_{-\infty}^0 \frac{1}{\sqrt{\pi}} e^{-y^2} dy + \int_0^{x'} \frac{1}{\sqrt{\pi}} e^{-y^2} dy$$

$$\begin{aligned}
&= \int_{-\infty}^0 \frac{1}{\sqrt{\pi}} e^{-y^2} dy + \int_0^{\infty} \frac{1}{\sqrt{\pi}} e^{-y^2} dy - \int_0^{\infty} \frac{1}{\sqrt{\pi}} e^{-y^2} dy + \int_0^{x'} \frac{1}{\sqrt{\pi}} e^{-y^2} dy \\
&= \int_{-\infty}^{\infty} \frac{1}{\sqrt{\pi}} e^{-y^2} dy - \int_0^{\infty} \frac{1}{\sqrt{\pi}} e^{-y^2} dy + \int_0^{x'} \frac{1}{\sqrt{\pi}} e^{-y^2} dy \\
&= 1 - \frac{1}{2} + \frac{1}{2} \operatorname{erf}(x') \\
&= 1 - \frac{1}{2} \left(1 - \frac{1}{2} \operatorname{erf}(x')\right) \\
&= 1 - \frac{1}{2} \operatorname{erf}(x') \\
\text{Prob(CSC)} &= \int_{-\infty}^{\infty} \frac{1}{\sqrt{\pi}} e^{-z^2} \left[1 - \frac{1}{2} \operatorname{erfc}(x')\right]^{M-1} dz \tag{A8}
\end{aligned}$$

For M=2

$$\begin{aligned}
\text{Prob(CSC)} &= \int_{-\infty}^{\infty} \frac{1}{\sqrt{\pi}} e^{-z^2} \left[1 - \frac{1}{2} \operatorname{erfc}(x')\right]^1 dz \\
&= \int_{-\infty}^{\infty} \frac{1}{\sqrt{\pi}} e^{-z^2} dz - \frac{1}{2} \int_{-\infty}^{\infty} \frac{1}{\sqrt{\pi}} e^{-z^2} \operatorname{erfc}(x') dz \\
&= 1 - \frac{1}{2} \int_{-\infty}^{\infty} \frac{1}{\sqrt{\pi}} e^{-z^2} \operatorname{erfc}(x') dz \tag{A9}
\end{aligned}$$

$$\text{Prob}_{M\text{-PPM}}(\text{bit-error}) = N_{\text{BS}}(1 - \text{Prob(CSC)})$$

$$= \frac{N_{\text{BS}}}{2\sqrt{\pi}} \int_{-\infty}^{\infty} e^{-z^2} \operatorname{erfc}(x') dz \tag{A10}$$

For M=4

$$\text{Prob(CSC)} = \int_{-\infty}^{\infty} \frac{1}{\sqrt{\pi}} e^{-z^2} \left[1 - \frac{1}{2} \operatorname{erfc}(x')\right]^3 dz$$

$$\begin{aligned}
&= \int_{-\infty}^{\infty} \frac{1}{\sqrt{\pi}} e^{-z^2} \left[1 - \frac{3}{2} \operatorname{erfc}(x') + \frac{3}{4} (\operatorname{erfc}(x'))^2 - \frac{1}{8} (\operatorname{erfc}(x'))^3 \right] dz \\
&= \int_{-\infty}^{\infty} \frac{1}{\sqrt{\pi}} e^{-z^2} dz - \frac{1}{2\sqrt{\pi}} \int_{-\infty}^{\infty} e^{-z^2} (3\operatorname{erfc}(x') - \frac{3}{2} (\operatorname{erfc}(x'))^2 + \frac{1}{4} (\operatorname{erfc}(x'))^3) dz \\
&= 1 - \frac{1}{2\sqrt{\pi}} \int_{-\infty}^{\infty} e^{-z^2} (3\operatorname{erfc}(x') - \frac{3}{2} (\operatorname{erfc}(x'))^2 + \frac{1}{4} (\operatorname{erfc}(x'))^3) dz \quad (\text{A11})
\end{aligned}$$

Therefore,

$$\begin{aligned}
&\text{Prob}_{\text{M-PPM}}(\text{bit-error}) = N_{\text{BS}} (1 - \text{Prob}(\text{CSC})) \\
&= \frac{N_{\text{BS}}}{2\sqrt{\pi}} \int_{-\infty}^{\infty} e^{-z^2} (3\operatorname{erfc}(x') - \frac{3}{2} (\operatorname{erfc}(x'))^2 + \frac{1}{4} (\operatorname{erfc}(x'))^3) dz \quad (\text{A12})
\end{aligned}$$

For M=8

$$\begin{aligned}
\text{Prob}(\text{CSC}) &= \int_{-\infty}^{\infty} \frac{1}{\sqrt{\pi}} e^{-z^2} \left[1 - \frac{1}{2} \operatorname{erfc}(x') \right]^7 dz \\
&= \int_{-\infty}^{\infty} \frac{1}{\sqrt{\pi}} e^{-z^2} \left[1 - \frac{7}{2} \operatorname{erfc}(x') + \frac{21}{4} (\operatorname{erfc}(x'))^2 - \frac{35}{8} (\operatorname{erfc}(x'))^3 + \frac{35}{8} (\operatorname{erfc}(x'))^4 \right. \\
&\quad \left. - \frac{21}{32} (\operatorname{erfc}(x'))^5 + \frac{7}{64} (\operatorname{erfc}(x'))^6 - \frac{7}{128} (\operatorname{erfc}(x'))^7 \right] dz \\
\text{Prob}(\text{CSC}) &= \int_{-\infty}^{\infty} \frac{1}{\sqrt{\pi}} e^{-z^2} dz - \frac{1}{2\sqrt{\pi}} \int_{-\infty}^{\infty} e^{-z^2} \left[(7\operatorname{erfc}(x') - \frac{21}{2} (\operatorname{erfc}(x'))^2 + \frac{35}{4} (\operatorname{erfc}(x'))^3) \right. \\
&\quad \left. - \frac{35}{8} (\operatorname{erfc}(x'))^4 + \frac{21}{16} (\operatorname{erfc}(x'))^5 - \frac{7}{32} (\operatorname{erfc}(x'))^6 + \frac{7}{64} (\operatorname{erfc}(x'))^7 \right] dz \\
&= 1 - \frac{1}{2\sqrt{\pi}} \int_{-\infty}^{\infty} e^{-z^2} \left[(7\operatorname{erfc}(x') - \frac{21}{2} (\operatorname{erfc}(x'))^2 + \frac{35}{4} (\operatorname{erfc}(x'))^3 - \frac{35}{8} (\operatorname{erfc}(x'))^4 \right. \\
&\quad \left. + \frac{21}{16} (\operatorname{erfc}(x'))^5 - \frac{7}{32} (\operatorname{erfc}(x'))^6 + \frac{7}{64} (\operatorname{erfc}(x'))^7 \right] dz \quad (\text{A13})
\end{aligned}$$

APPENDIX B
HERMITE POLYNOMIAL

Hermite polynomial for orthogonal is given by

$$H_n(x) = \int_{-\infty}^{\infty} e^{-x^2} f(x) dx = \sum_{i=1}^n w_i f(x_i) + R_n$$

Abscissas x_i is the i^{th} zero of $H_n(x)$.

Weights:

$$\frac{2^{n-1} n! \sqrt{\pi}}{n^2 [H_{n-1}(x_i)]^2}$$

Remainder:

$$R_n = \frac{n! \sqrt{\pi}}{2^n (2n)!} f^{(2n)}(\epsilon) \quad (-\infty < \epsilon < \infty)$$

ABSCISSAS AND WEIGHT FACTORS FOR HERMITE INTEGRATION

$$\int_{-\infty}^{\infty} e^{-z^2} f(x) dx = \sum_{i=1}^n w_i f(x_i)$$

$$\int_{-\infty}^{\infty} g(x) dx = \sum_{i=1}^n w_i e^{-z_i^2} g(x_i)$$

Abscissas = $+x_i$ (Zeros of Hermite Polynomials)

Weight Factors = w_i

n	$\pm x_i$	w_i	$w_i e^{-z_i^2}$
2	0.70710 67811 86548	(-1)8.86226 92545 28	1.46114 11826 611
3	0.00000 00000 00000	(0) 1.18163 59006 04	1.18163 59006 037
	1.22474 48713 91589	(-1) 2.95408 97515 09	1.32393 11752 136
4	0.52464 76232 75290	(-1)8.04914 09000 55	1.0549644828950
	1.65068 01238 85785	(-2)8.13128 35447 25	1.24022 58176 958
5	0.00000 00000 00000	(-1)9.45308 72048 29	0.94530 87204 829
	0.95857 24646 13819	(-1)3.93619 32315 22	0.98658 09967 514
	2.02016 28704 56086	(-2)1.99532 42059 05	1.18148 86255 360
6	0.43607 74119 27617	(-1)7.24629 59522 44	0.87640 13344 362
	1.33584 90740 13697	(-1)1.57067 32032 29	0.93558 05576 312
	2.35060 49736 74492	(-3)4.53000 99055 09	1.13690 83326 745
7	0.00000 00000 00000	(-1)8.10264 61755 68	0.81026 46175 568
	0.81628 78828 58965	(-1)4.25607 25261 01	0.82868 73032 836
	1.67355 16287 67471	(-2)5.45155 82819 13	0.89718 46002 252
	2.65196 23968 35233	(-4)9.71781 24509 95	1.10133 07296 103
8	0.38118 69902 07322	(-1)6.61147 01255 82	0.76454 41286 517
	1.15719 78828 58965	(-1)2.07802 32581 49	0.79289 00483 864
	1.98165 65565 95843	(-2)1.70779 83007 41	0.86675 26065 634
	2.93063 74020 57244	(-4)1.99604 07221 14	1.07193 01442 480
9	0.00000 00000 00000	(-1)7.20235 21560 61	0.72023 52156 061
	0.72355 10187 52838 26	(-1)4.32651 55900	0.73030 24527 451
	1.46855 32892 16668	(-2)8.84745 27394 38	0.76460 81250 946
	2.26658 05845 31843	(-3)4.94362 42755 37	0.84175 27015 787
	3.19099 32017 81528	(-9)3.96069 77263 26	1.04700 35809 767
10	0.34290 13272 23705	(-1)6.10862 63373 53	0.88708 18539 513
	1.03661 08297 89514	(-1)2.40138 61108 23	0.70329 63231 049
	1.75668 36492 99882	(-2)3.38743 94455 48	0.74144 19319 436
	2.53273 16742 32790	(-3)1.34364 57464 81	0.82066 61264 048
	3.4365 91188 37738	(-6)7.64043 28552 33	1.02545 16913 657

12	0.31424 03762 54359 0.94778 83912 40164 1.59768 26351 52605 2.27950 70805 0060 3.02063 70251 20890 3.88972 48978 69782	(-1)5.70135 23626 25 (-1)2.60492 31026 42 (-2)5.16079 85615 88 (-3)3.90539 05846 29 (-5)8.57368 70435 88 (-7)2.65855 16843 56	0.62930 78743 695 0.63962 12320 203 0.6266 27732 669 0.70522 03661 122 0.78644 39394633 0.98969 90470 923
16	0.27348 10461 3815 0.82295 14491 4466 1.38025 85391 9888 1.95178 79909 1625 2.54820 21578 4748 3.17699 91619 7996 3.86994 79048 6012 4.68873 89393 0582	(-1)5.07929 47901 66 (-1)2.80647 45852 85 (-2)8.38100 41398 99 (-2)1.28803 11535 51 (-4)9.32284 00862 42 (-5)2.71186 00925 38 (-7)2.32098 08448 65 (-10)2.65480 74740 11	0.54737 52050 378 0.55244 19573 657 0.56321 78290 882 0.58124 72754 009 0.60973 6982 560 0.65575 56728 761 0.73824 56222 777 0.93687 44928 841
20	0.24534 07083 009 1.23407 62153 953 1.73853 77121 166 2.25497 40020 893 2.78880 60584 281 3.34785 45673 832 3.94476 40401 156 4.60368 24495 507 5.38748 0900 112	(-1)4.62243 66960 06 (-1)1.09017 20602 00 (-2)2.48105 20887 46 (-3)3.24377 33422 38 (-4)2.28338 63601 63 (-6)7.80255 64785 32 (-7)1.08606 93707 69 (-10)4.39934 0992273 (-13)2.22939 36455 34	0.49092 15006 667 0.49992 08713 363 0.50967 90271 175 0.52408 03509 486 0.54485 17423 644 0.57526 24428 525 0.62227 86961 914 0.70433 29611 769 0.89859 19614 532

